View metadata, citation and similar papers at core.ac.uk

brought to you by CORE

provided by CORE

Wright State University

CORE Scholar

Mathematics and Statistics Faculty Publications

Mathematics and Statistics

1-2017

Flexibility of Projective-Planar Embeddings

John Maharry

Neil Robertson

Vaidy Sivaraman

Dan Slilaty
Wright State University - Main Campus, daniel.slilaty@wright.edu

Follow this and additional works at: https://corescholar.libraries.wright.edu/math

Part of the Applied Mathematics Commons, Applied Statistics Commons, and the Mathematics Commons

Repository Citation

Maharry, J., Robertson, N., Sivaraman, V., & Slilaty, D. (2017). Flexibility of Projective-Planar Embeddings. *Journal of Combinatorial Theory, Series B, 122*, 241-300.
https://corescholar.libraries.wright.edu/math/310

This Article is brought to you for free and open access by the Mathematics and Statistics department at CORE Scholar. It has been accepted for inclusion in Mathematics and Statistics Faculty Publications by an authorized administrator of CORE Scholar. For more information, please contact library-corescholar@wright.edu.

Flexibility of Projective-Planar Embeddings

John Maharry *
Department of Mathematics
The Ohio State University
Columbus, OH USA

Neil Robertson †
Department of Mathematics
The Ohio State University
Columbus, OH USA

Vaidy Sivaraman ‡
Department of Mathematical Sciences
State University of New York at Binghamton
Binghamton, NY USA

Daniel Slilaty §
Department of Mathematics
Wright State University
Dayton, OH USA

June 17, 2016

Abstract

Given two embeddings σ_1 and σ_2 of a labeled nonplanar graph in the projective plane, we give a collection of maneuvers on projective-planar embeddings that can be used to take σ_1 to σ_2.

Keywords: *Projective plane, projective-planar graph, embedding, reembedding, flexibility, twisting operations, Wagner graph, Petersen graph, signed-graphic matroid.*

1 Introduction

Consider a labeled connected graph G with two cellular embeddings σ_1 and σ_2 in the projective plane. In the case that G is planar, it is shown in [8] that there are embeddings $\psi_1, \ldots, \psi_n$ of G (with $\sigma_1 = \psi_1$ and $\sigma_2 = \psi_n$) such that ψ_{i+1} is obtained from ψ_i by one from a list of given maneuvers of a graph embedded in the projective plane. In this paper we solve the same problem for the case when G is not planar. This problem has previously been considered in [10], [17] and [20]; however, each contain errors. We will discuss these and related results (which are also mentioned in the next paragraph) in Section 6.

There are many results in the literature concerning the reembeddings of graphs in various surfaces; in particular, results relating the number of reembeddings to representativity (i.e., face width). The classical result of Whitney ([21, 22] or [9, Thm.2.6.8]) is that any 3-connected planar graph G has a unique embedding in the plane. Robertson and Vitray [13] showed that for any orientable surface

*E-mail address: `maharry@math.ohio-state.edu`
†E-mail address: `robertso@math.ohio-state.edu`
‡E-mail address: `vaidy@math.binghamton.edu`
§E-mail address: `daniel.slilaty@wright.edu`. Work partially supported by a grant from the Simons Foundation #246380.

S of genus g, any 3-connected graph G embedded in Σ with representativity at least $2g+3$ has a unique embedding in that surface. Mohar [6] and Seymour and Thomas [15] lowered this bound to $c\log(g)/\log(\log(g))$. Robertson, Zha, and Zhao [14] showed that, other than $C_4 \times C_4$ and a small number of graphs contracting to $C_4 \times C_4$, any graph with an embedding of representativity at least 4 in the torus has a unique embedding in the torus. Robertson and Mohar [7] have shown that for any surface S, there is a number $f(S)$ such that for any 3-connected graph G, there are at most $f(S)$ distinct embeddings of G in S with representativity at least 3. They also give examples to show that no such bound exists depending only on the surface for highly-connected 2-representative embeddings. As corollaries to our main result (in Section 6) we will reprove the following two related results from [10] for projective-planar embeddings. First, for any 3-connected graph with an embedding of representativity at least 4 in the projective plane, that embedding is the only embedding (Theorem 6.1). Second, other than K_6, for any 5-connected graph with an embedding of representativity 3 in the projective plane, that is the only embedding (Theorem 6.2).

Before we state our main result, we would also like to mention a relationship between this problem and a problem on signed graphs. If Σ_1 and Σ_2 are two signed graphs with the same labeled edge set, then when does $M(\Sigma_1) = M(\Sigma_2)$? (Here $M(\Sigma_i)$ is the frame matroid of the signed graph Σ_i. See [23] for an introduction to signed graphs and their matroids.) Since the relationship between different representations of the same matroid is very important in matroid theory, an answer to this question is desirable. In [16] it is shown that if $M(\Sigma_1)$ is connected and not graphic, then $M(\Sigma_1) = M^*(G)$ for some ordinary graph G if and only if Σ_1 and G are topological duals in the projective plane. So if $M(\Sigma_1) = M(\Sigma_2) = M^*(G)$ is 3-connected, then Whitney's 2-Isomorphism Theorem (see, for example, [11, Sec.5.3]) tells us that G is the only ordinary graph that represents $M^*(G)$. Thus the difference between Σ_1 and Σ_2 is just that they are duals of two distinct embeddings of G in the projective plane. Hence this problem of signed-graphic matroid isomorphism contains the reembedding problem of ordinary graphs in the projective plane as a special case.

In Section 2, we will define three operations on a graph embedded in the projective plane: Q-Twists, P-Twists, and W-Twists. (Here Q, P, and W stand for quadrilateral, Petersen, and Whitney.) Our main result is Theorem 1.1. This result is the analogue to Whitney's result ([21, 22] or [9, Thm.2.6.8]) that two different embeddings of the same graph in the plane are related by a sequence of W-Twists.

Theorem 1.1. *Let G be a connected, nonplanar graph. If σ_1 and σ_2 are two embeddings of G on the projective plane, then there exists a sequence of Q-Twists, P-Twists, and W-Twists taking σ_1 to σ_2.*

Our main lemma to the proof of Theorem 1.1 is Lemma 1.2, the proof of which requires the vast majority of this paper. We say that a graph G is *k-connected* when G has no separating set of fewer than k vertices and the girth of G is at least k, i.e., Tutte's version of connectivity.

Lemma 1.2. *Let G be a 3-connected, nonplanar graph. If σ_1 and σ_2 are two embeddings of G on the projective plane, then there exists a sequence of Q-Twists and P-Twists taking σ_1 to σ_2.*

A natural approach to proving Lemma 1.2 would be to find a topological subgraph H of G with known flexibility in the projective plane and then examine the H-bridges and how they behave under the flexibility of H. A natural candidate for H would be $K_{3,3}$-subdivision because G is guaranteed to contain a $K_{3,3}$-subdivision unless $G \cong K_5$. However, it seems to us that such an approach is not feasible and so we start with a subgraph H that is a subdivision of the Wagner graph V_8. The Wagner graph V_8 (also called the 4-rung Möbius Ladder) is obtained from an 8-cycle on vertices $v_1, v_2, \ldots, v_8$ by adding four v_iv_{i+4}-chords. In any projective-planar embedding of V_8 its octagon must be embedded contractibly; with $K_{3,3}$ there is no such cycle that is guaranteed to be contractible. This property of V_8 makes a proof of Lemma 1.2 starting with a V_8-subdivision tractable as the reader will see in Section 4. Thus we split the proof of Lemma 1.2 into two cases: where G contains a V_8-minor (Section 4) and where G is V_8-free (Section 5). The V_8-free case is facilitated by Theorem 1.3 which is a result known independently to both Robertson and Kelmans since at least 1982. A proof of this result was finally published by Robertson and Maharry in [5]. One might ask whether one could extend the techniques of Section 4 to graphs with a $K_{3,3}$-minor but no V_8-minor in order to avoid using Theorem 1.3. We suspect that such an approach might just reproduce much of the details of a proof of Theorem 1.3.

Theorem 1.3. *Let G be an internally 4-connected graph with no V_8-minor. Then G belongs to one of the following families:*

1. *planar graphs,*
2. *subgraphs of double wheels (i.e., there exist two adjacent vertices a, b of G such that $G \setminus \{a, b\}$ is a cycle),*
3. *graphs with a 4-vertex edge cover (i.e., there exist four vertices a, b, c, d of G such that $V(G) \setminus \{a, b, c, d\}$ is edgeless),*
4. *the line graph of $K_{3,3}$, and*
5. *graphs with seven or fewer vertices.*

2 Twisting Operations

A *Q-Twist* is one of the operations described in this paragraph. The *full* Q-Twist operation *hinged* at $1, 2, 3, 4$ and *latched* at A, B is the operation shown (from two viewpoints) in Figure 1 for a graph embedded in the projective plane. One can identify and/or delete hinges and latches of the full Q-Twist to obtain a *degenerate* Q-Twist. Several degenerate Q-Twists are shown in Figure 2. For the rightmost degenerate Q-Twist, when the light grey block is a single edge we often refer to this operation as *flipping* an edge. It is worth noting that Q-Twist operations (both and full and degenerate) apply to embeddings of representativity at most three and that only the full Q-Twist (and not any of the degenerate Q-Twists) can be applied to embeddings of representativity exactly three.

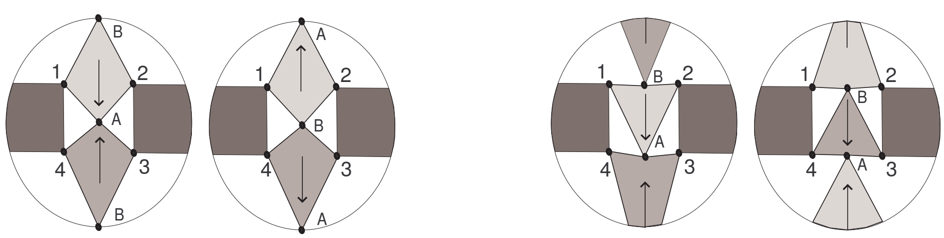

Figure 1.

The Q-Twist operation hinged at $1, 2, 3, 4$ and latched at A, B.

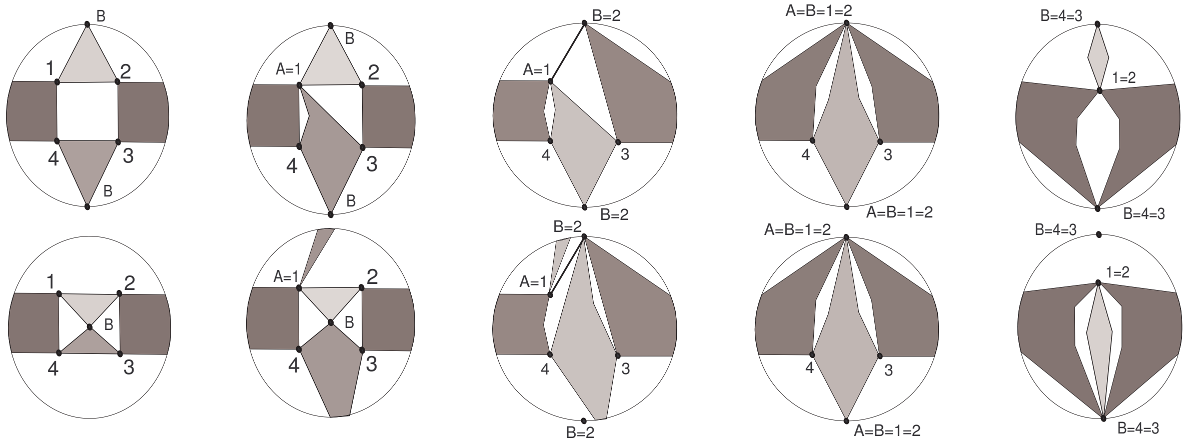

Figure 2.

Various degenerate Q-Twists.

A *P-Twist* is one of the operations described in this paragraph. The *full* P-Twist is the operation shown in the first column of Figure 3 for a graph embedded in the projective plane. The second and third columns of Figure 3 are different drawings of the P-Twist. We refer to these three drawings, respectively, as the 'bowtie', 'central', and 'pentagonal' views. A *degenerate* P-Twist is obtained from a full P-Twist by contracting a triangular patch or by contracting one side of a triangular patch. In Figure 4 we show three typical degenerate P-Twists all obtained from the bowtie view of the full P-Twist. The first is obtained by contracting patches 2,4,8,9, the second is obtained by contracting patch 5, and the third is obtained from the second by contracting the dark patches to two edges as labeled

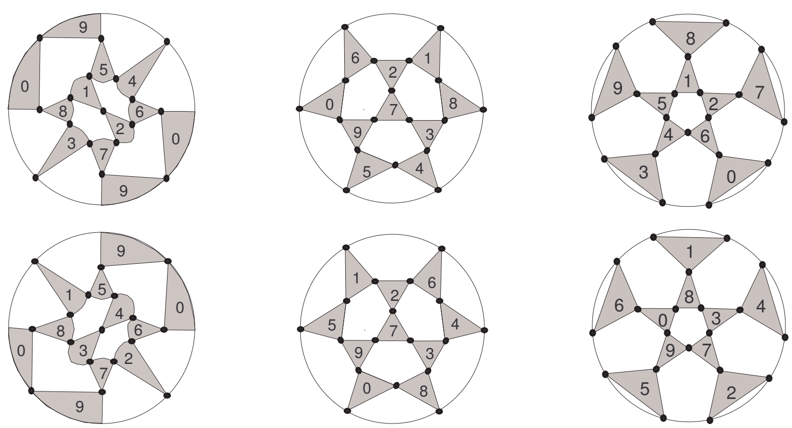

Figure 3.

The three views of the P-Twist

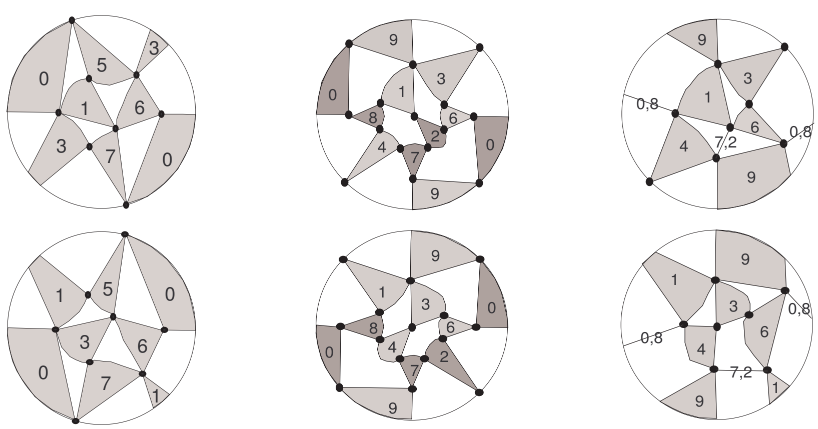

Figure 4.

Various degenerate P-Twists.

It is worth noting that the full P-Twist without the shading in the triangles is the line graph of the Petersen graph, call it $L(P)$ where P is the Petersen graph. One can check that there are exactly two distinct embeddings of P. Now since P is cubic, each embedding of P extends uniquely to an embedding of $L(P)$ and any embedding of $L(P)$ comes from an embedding of P. Hence there are only two embeddings of $L(P)$ and these embeddings are related by the full P-Twist. Furthermore, the two embeddings cannot be related by a Q-Twist (or a sequence of Q-Twists) because in a Q-Twist there are at most 6 vertices whose rotation of edges (up to reversal) is changed by the operation. In the two embeddings of $L(P)$ changes in rotation occurs at all 15 vertices.

Finally, a *W-Twist* hinged on vertices A and B is the operation shown in Figure 5. A degenerate W-Twist is defined as the operation that arises if we delete vertex B from the figure.

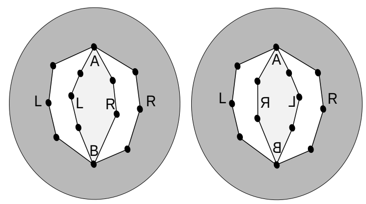

Figure 5.

The W-Twist

3 Proof of Theorem 1.1

In this section we prove Theorem 1.1 assuming Lemma 1.2. A graph G is said to be *k-connected* when G has at least k vertices, no separating set of fewer than k vertices, and girth at least k (i.e., we are using "Tutte connectivity" rather than the weaker, yet more standard, definition of connectivity). Let G and H be graphs on disjoint vertex sets, each with a proper K_t-subgraph. Define $G \oplus_t H$ to be a graph obtained by identifying the K_t-subgraphs and then deleting some, none, or all of the edges of the K_t-subgraph. This operation is called a *t-sum* of G and H. If G is 2-connected, but not 3-connected, then $G = G_1 \oplus_2 G_2$ where each G_i is a proper minor of G and is 2-connected. If G is 3-connected but not 4-connected, then $G = G_1 \oplus_3 G_2$ where the following are true.

(1) Each G_i is 3-connected aside perhaps from double edges along the triangle of summation. These double edges can be avoided, however, by appropriately defining the 3-sum.

(2) Each G_i is a minor of G with $|E(G_i)| < |E(G)|$ except in the case that one of G_1 and G_2 is K_4 and the 3-sum $G = G_1 \oplus_3 G_2$ deletes all edges of the summing triangle.

In (2) the 3-sum is called a ΔY-operation. If G is 3-connected and every 3-separation of G yields only an expression of G as a 3-sum that is a ΔY-operation, then G is said to be *internally 4-connected.*

Our proof will proceed by induction on $|V(G)| + |E(G)|$. In the base case $|V(G)| + |E(G)| = 15$ and so $G \cong K_5$ or $K_{3,3}$ which are both 3-connected. The result then follows by Lemma 1.2. Suppose now that $|V(G)| + |E(G)| > 15$ and G is connected but not 3-connected (the 3-connected case follows by Lemma 1.2).

Proposition 3.1. *If G is connected, nonplanar, projective planar, and not 3-connected, then $G = H \oplus_t P$ for $t \in \{1, 2\}$ where P is planar and H is not.*

Proof. Given that G is connected but not 3-connected, $G = H \oplus_t P$ for $t \in \{1, 2\}$. Since planarity is closed under 1-sums and 2-sums, then without loss of generality H is not planar. It must be that P is planar because otherwise G will contain one of the twelve excluded minors for projective planarity that are not 3-connected. A proof for $t = 1$ is evident and a proof for $t = 2$ can be found in [12, §3]. $\square$

Hence we can assume that $G = H \oplus_t P$ for $t \in \{1, 2\}$ where P is planar and H is not. If $t = 2$, then let $\{x, y\}$ be the vertices of the 2-separation of G and e be the (x, y)-edge of H and P. Rechoose H and P so that P has a minimal number of edges, in which case the only possible 2-separation of P at $\{x, y\}$ would be from a single pair of parallel (x, y)-edges. So if σ_1 and σ_2 are distinct embeddings of G in the projective plane, these restrict to embeddings $\sigma_i|_H$ and $\sigma_i|_P$. By the restriction on 2-separations in P, the embedding $\sigma_i|_P$ is either inside a disk or inside a disk aside from one or two (x, y)-edges. These (x, y)-edges can be flipped (i.e., a degenerate Q-Twist on a single edge) with respect to an embedding of the entirety of G so that the induced embedding on P is now within a disk. Now by induction, there is a sequence of Q-, P- and W-twists that takes $\sigma_1|_H$ to $\sigma_2|_H$. Also by Whitney's Theorem ([21, 22] or [9, Thm.2.6.8]) and by flipping, there is a sequence of Q-Twists and W-twists that takes $\sigma_1|_P$ to $\sigma_2|_P$. These operations take σ_1 to σ_2. The proof for $t = 1$ is similar.

4 Proof of Lemma 1.2 for graphs with a V_8-minor

Given a subgraph H of a graph G, we assume the reader is familiar with the terms *subdivision, branch, branch vertex, H-bridge, local H-bridge,* and *vertices of attachment* as defined in [9].

The *n-rung Möbius ladder* V_{2n} is the graph obtained from the cycle on vertex set $\{1, 2, \ldots, 2n\}$ by adding an $(i, n+i)$-edge for each $1 \le i \le n$. Note that $V_4 \cong K_4$ and $V_6 \cong K_{3,3}$. In this section we prove Lemma 1.2 in the case that G has a V_{2n}-minor for some $n \ge 4$.

Let ν_0 be the canonical projective-planar embedding of V_{2n} with a facial $2n$-cycle. Let ν_i with $i \in \{1, 2, \ldots, n\}$ be the embedding obtained from ν_0 by flipping in the $(i, i+n)$-chord. (Figure 6 shows the embeddings ν_0 and ν_4 for V_8.) For $n \ge 4$, one can check that there is no embedding of V_{2n} in which the $2n$-cycle is noncontractible. Hence $\nu_0, \nu_1, \ldots, \nu_n$ are all of the embeddings of V_{2n} for $n \ge 4$.

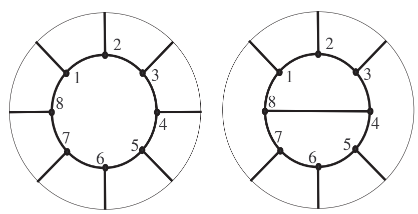

Figure 6.

Up to relabeling there are two embeddings of V_8.

Now let G be a 3-connected graph with two distinct embeddings on the projective plane, σ_1 and σ_2. Let H be a V_{2n}-subdivision contained in G with n a maximum. Since G is 3-connected we can now rechoose H so that it has no local H-bridges (see [2] or [9, Lemma 6.2.1]). (An H-bridge of G is local if all of its vertices of attachment lie on a single branch of H.) Hence we can assume that any H-bridge has two vertices of attachment not on the same branch. Also, any branch of H that can be chosen to be a single edge is chosen as such. Let $\gamma_{i,j}$ be the branch of H corresponding to the (i, j)-edge of V_{2n} and let C_H be the cycle in H corresponding to the $2n$-cycle of V_{2n}. We refer to $\gamma_{i,i+n}$ as a chord of C_H even though it may be subdivided to have length greater than one.

Let $\sigma_1|_H$ and $\sigma_2|_H$ be the restrictions of the two embeddings σ_1 and σ_2 to H. Without loss of generality, we can split the problem into the following five cases. In Case 1, suppose $\sigma_1|_H = \sigma_2|_H = \nu_0$. In Case 2, suppose $\sigma_1|_H = \nu_0$ and $\sigma_2|_H = \nu_1$. In Case 3, suppose $\sigma_1|_H = \sigma_2|_H = \nu_1$. In Case 4, suppose $\sigma_1|_H = \nu_1$ and $\sigma_2|_H = \nu_2$. Finally, in Case 5, suppose $\sigma_1|_H = \nu_1$ and $\sigma_2|_H = \nu_k$ with $k \in \{3, n-1\}$.

Before beginning our case analysis, we will describe some general principles that we will use in all (or most) of the cases.

Two embeddings of G in a closed surface S are the same if and only if they have the same facial boundary walks. Consider any embedding ψ of G in the projective plane. Since any embedding of $H \subseteq G$ is 2-representative, every facial boundary of H is a cycle in G. Now let A be a facial boundary cycle of H of length ℓ, let $B_1, \ldots, B_t$ be the H-bridges of G that are embedded inside of A, and let K be the graph $K_{1,\ell}$ with degree-1 vertices to be attached to the vertices of A. Since G is 3-connected, we get that $K \cup A \cup B_1 \cup \cdots \cup B_t$ is a 3-connected planar graph. As such the facial cycles of $K \cup A \cup B_1 \cup \cdots \cup B_t$ are uniquely determined. Thus an embedding ψ of G in the projective plane is uniquely determined by which face of H a given bridge is embedded in.

Since C_H is contractible in all embeddings of H, we say that an H-bridge B is *reembedded* with respect to σ_1 and σ_2 if B is inside the disk region of C_H in exactly one of the embeddings. Otherwise, we say B is *fixed* with respect to σ_1 and σ_2. We call B *reembeddable* when there is an embedding σ_2' of $H \cup B$ with $\sigma_2'|_H = \sigma_2|_H$ such that B is reembedded with respect to σ_1 and σ_2'. Evidently any reembedded bridge is reembeddable and a fixed bridge may or may not be reembeddable.

Given σ_1 and σ_2, let $\overline{H}$ be the subgraph of H with edges and interior vertices of the chords of C_H that are flipped relative to σ_1 and σ_2 removed. We call this the *fixed subgraph* of H. Note that in Cases 1 and 3, $\overline{H} = H$; in Case 2, $\overline{H}$ is a V_{2n-2}-subdivision with $2n-2 \geq 6$; and in Cases 4 and 5, $\overline{H}$ is a V_{2n-4}-subdivision with $2n-4 \geq 4$. In Case 3, $\sigma_1|_{\overline{H}} = \sigma_2|_{\overline{H}} = \nu_1$ and in all the remaining cases, $\sigma_1|_{\overline{H}} = \sigma_2|_{\overline{H}} = \nu_0$. So now in Cases 1–3 (because $2n-2 \geq 6$) the face of $\overline{H}$ in which a given H-bridge B is embedded in σ_k is uniquely determined by whether B is interior or exterior to C_H in σ_k. Thus the embeddings σ_1 and σ_2 when restricted to $\overline{H} \cup B$ are the same (i.e., have the same facial boundary walks) if and only if B is a fixed bridge. In Cases 4 and 5 with $n \geq 5$, we get the same result for H-bridges and $\overline{H}$. In Case 4 with $n = 4$, we do not, a priori, get this result for the faces of B in $\overline{H}$. The only time this might fail is when B has all of its attachments on the $\gamma_{3,7}$- and $\gamma_{4,8}$-chords because there are exactly two faces in $\overline{H}$ that are exterior to C_H and B may be embedded in either one. In this case, however, since one of the faces of $\overline{H}$ exterior to C_H is also a face of H, this cannot happen. So again in Case 4 we get that σ_1 and σ_2 restricted to $\overline{H} \cup B$ are the same if and only if B is a fixed bridge. In Case 5 with $n = 4$, this possibility does indeed happen (e.g., with the two embeddings of the Petersen graph relative to any V_8-subdivision). Therefore in all cases save Case 5 with $n = 4$, the embeddings σ_1 and σ_2 restricted to $\overline{H}$ and its fixed H-bridges are the same embeddings; that is, the difference between σ_1 and σ_2 is described exactly by which H-bridges are reembedded. In Case 5 with $n = 4$, we do not use the terms fixed and reembedded.

Two H-bridges in G with attachments on a cycle C are called *overlapping* with respect to C if they share three common attachments on C or have pairs of alternating attachments on C. Also we say that B *belongs* to face F of H in ν_i if all of its attachments are on F. Note that if two H-bridges B_1 and B_2 both belong to F and are overlapping with respect to F then one of B_1 and B_2 must belong to some other face as well.

The basic strategy for each case (except Case 5 with $n = 4$) is to first identify what the reembeddable H-bridges are and then to define a sequence of Q-Twists taking σ_1 to σ_2. In this proof for graphs with V_8-minors, P-Twists only appear in Case 5 with $n = 4$. When defining a potential twist we must always verify that there are no bridges (fixed or otherwise) that obstruct it.

Case 1 Note that any H-bridge B is reembeddable if and only if all of the attachments of B are on $\gamma_{i,i+1} \cup \gamma_{i+n,i+1+n}$ for some $i \in \{1, 2, \ldots, n\}$ and there are no two vertex-disjoint paths in B connecting $\gamma_{i,i+1}$ to $\gamma_{i+n,i+1+n}$. So then each reembeddable bridge belongs to C_H and the other face of $\sigma_1|_H = \sigma_2|_H$ with $\gamma_{i,i+1} \cup \gamma_{i+n,i+n+1}$ on its boundary. Call this latter face F_i.

The note in the previous paragraph implies that if B is reembeddable, then either:

- B is a single edge with one endpoint on $\gamma_{i,i+1}$ and the other on $\gamma_{n+i,n+i+1}$,
- B has exactly one attachment on either $\gamma_{i,i+1}$ or $\gamma_{i+n,i+n+1}$ and at least two attachments on the other as in the two embeddings on the left in Figure 7,
- or B has a cut vertex in its interior as in the two embeddings on the right in Figure 7. (The existence of this cut vertex follows from Menger's Theorem and the fact that the are no two disjoint paths in B from $\gamma_{i,i+1}$ to $\gamma_{i+n,i+1+n}$.)

We will call single-edge bridges I-type bridges, the second kind V-type bridges, and the last kind X-type bridges. For V-type bridges, let the singular attachment be called its *apex*.

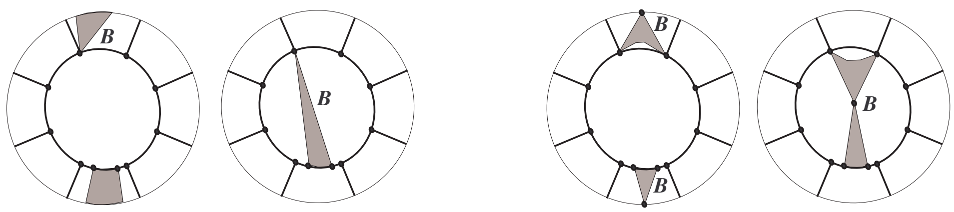

Figure 7.

Reembeddable bridges with all attachments on H.

As V_{2n} was taken with n maximal, we get the following restrictions on these three reembeddable types of bridges. For I-type bridges, at least one attachment must be a branch vertex of H. For V-type bridges, either the apex is a branch vertex of H or all of the non-apex attachments are branch vertices of H. These will be called V_{end}-type and V_{int}-type for apex on a branch vertex and apex in the interior of a branch, respectively. For X-type bridges, they cannot have interior attachments on both branches.

For a given face F_i, let $B_1, \ldots, B_k$ be the reembeddable bridges belonging to F_i that are pairwise non-overlapping with respect to C_H and interior to C_H in σ_j ($j \in \{1, 2\}$). The restrictions on the bridge structures in the previous paragraph yield the following possible configurations for $\gamma_{i,i+1} \cup \gamma_{i+n,i+n+1} \cup B_1 \cup \cdots \cup B_k$ inside C_H. If there is a V_{int}-type bridge in $\{B_1, \ldots, B_k\}$, then the remaining bridges in $\{B_1, \ldots, B_k\}$ must all be V_{end}-type and I-type and $\gamma_{i,i+1} \cup \gamma_{i+n,i+n+1} \cup B_1 \cup \cdots \cup B_k$ must be as on the left of Figure 8. If there is an X-type bridge in $\{B_1, \ldots, B_k\}$, then the remaining bridges in $\{B_1, \ldots, B_k\}$ must all be V_{end}-type and I-type and $\gamma_{i,i+1} \cup \gamma_{i+n,i+n+1} \cup B_1 \cup \cdots \cup B_k$ must be as in the second configuration in Figure 8. If there is no V_{int}-type or X-type bridge in $\{B_1, \ldots, B_k\}$, then $\gamma_{i,i+1} \cup \gamma_{i+n,i+n+1} \cup B_1 \cup \cdots \cup B_k$ have one of the two remaining types of configurations in Figure 8.

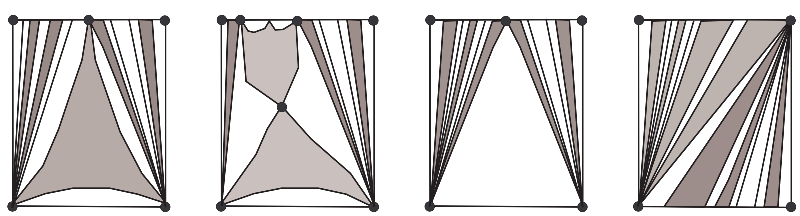

Figure 8.
Configurations of reembeddable non-overlapping bridges interior to C_H

A collection $\mathcal{F}$ of reembeddable V-type and I-type bridges sharing the same apex a, having all other attachments on the same branch of H, and all embedded in the same face of H is called a *fan* with apex a. We will call the first and last such attachments of $\mathcal{F}$ on this branch the *extreme feet of* $\mathcal{F}$. So now if $\mathcal{B}' \subseteq \{B_1, \ldots, B_k\}$ are bridges that are reembedded from σ_1 to σ_2, since there cannot be disjoint H-paths from $\gamma_{i,i+1}$ to $\gamma_{i+n,i+n+1}$ within the bridges of $\mathcal{B}'$, either $\mathcal{B}'$ is a single X-type bridge or a fan. As with V-type bridges, we further describe fans as *interior* fans or *endpoint* fans for when the apex is in the interior of a branch of H or on a branch vertex of H. Interior fans consist of at most one V_{int}-type bridge along with at most two I-type bridges. We do not consider a single I-type bridge as an interior fan. Thus the possible configurations of $\mathcal{B}'$ inside C_H are as in Figure 9.

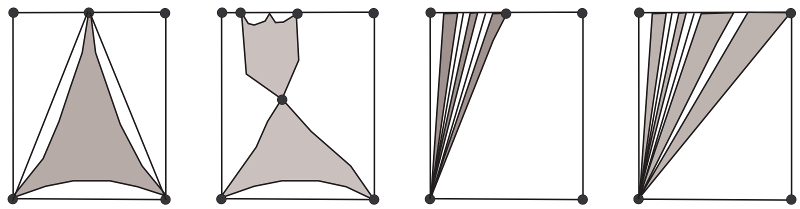

Figure 9.
Configurations of reembedded bridges interior to C_H

Since $\sigma_1 \neq \sigma_2$, there is some reembedded H-bridge: in Case 1.1 we assume that all of the reembedded bridges belong to one F_i, in Case 1.2 we assume that all of the reembedded bridges belong to exactly two distinct F_i's, in Case 1.3 we assume that all of the reembedded bridges belong to exactly three distinct F_i's, and in Case 1.4 we assume that there are reembedded bridges belonging to at least four distinct F_i's.

Case 1.1 Let $\mathcal{B}$ be the reembeddable bridges belonging to F_i and $\mathcal{B}' \subseteq \mathcal{B}$ be the ones that are actually reembedded. In Case 1.1.1 there is an X-type bridge in $\mathcal{B}'$. In Case 1.1.2 say there is no X-type bridge in $\mathcal{B}'$ and there is an interior fan in $\mathcal{B}'$. In Case 1.1.3 say there is no X-type and no interior fan in $\mathcal{B}'$.

Case 1.1.1 If there is an X-type bridge $X \in \mathcal{B}'$, then say without loss of generality X is interior to C_H in σ_1. Thus the remaining bridges in $\mathcal{B}'$ are all exterior to C_H in σ_1. Hence $\mathcal{B}' \setminus X$ is either a single X-type bridge or $\mathcal{B}' \setminus X$ is a fan with apex a. If $\mathcal{B}' \setminus X$ is a single X-type bridge, call it X'. Let $G' = H \cup X \cup X'$. We go from $\sigma_1|_{G'}$ to $\sigma_2|_{G'}$ by one full Q-Twist hinged on the extreme attachments of $X \cup X'$ on $\gamma_{i,i+1}$ and $\gamma_{i+n,i+n+1}$ and latched at the cut vertices in the interiors of X and X'. There can be no fixed H-bridges of G that obstruct extending this Q-Twist to all of G.

If $\mathcal{B}' \setminus X$ is a fan with apex a, then without loss of generality say that a is on path $\gamma_{i,i+1}$ and let α be the subpath of $\gamma_{i+n,i+n+1}$ connecting the extreme attachments of X. Let $\mathcal{B}''$ be the collection of bridges in $\mathcal{B}' \setminus X$ whose attachments on $\gamma_{i+n,i+n+1}$ are all not in the interior of α (see the left configuration in Figure 10). Each bridge B in $\mathcal{B}''$ is reembedded individually by degenerate Q-Twists to obtain embedding σ_1' as shown in the middle of Figure 10. (Note that there are no fixed H-bridges that can block these individual Q-Twists.) Now we can go from σ_1' to σ_2 by a Q-Twist hinged on the extreme attachments of $\mathcal{B}' \setminus \mathcal{B}''$ on $\gamma_{i,i+1} \cup \gamma_{i+n,i+n+1}$ and latched at the cut vertex in the interior of X and at a (see the last embedding in Figure 10) Again we note that there are no fixed H-bridges that block this final Q-Twist.

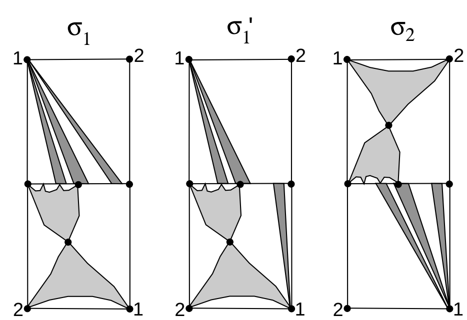

Figure 10.
Case 1.1.1: The lower quadrilateral is the interior of C_H.

Case 1.1.2 Let V be the reembedded interior fan. Without loss of generality, assume that V is interior to C_H in σ_1. If $\mathcal{B}' = V$, then we can go from σ_1 to σ_2 by a single degenerate Q-Twist. Otherwise, $\mathcal{B}' \setminus V$ is an interior or end fan inside F_i in σ_1. Let these be Cases 1.1.2.1 and 1.1.2.2.

Case 1.1.2.1 Let N be the interior fan in $\mathcal{B}' \setminus V$. Thus N consists of either a single V_{int}-type bridge along with $t \in \{0, 1, 2\}$ I-type bridges or exactly two I-type bridges. The first three configurations on the left in Figure 11 show the three possible configurations for $\mathcal{B}'$ with two V_{int}-type bridges along with a maximal collection of I-bridges. In each of these three cases we go from σ_1 to σ_2 by a single Q-Twist hinged on the extreme attachments of V and N and latched on the apices of V and N. No fixed bridges can block this single Q-Twist. There are other cases possible in which V_{int}-type and/or I-type bridges are not reembedded or are not there at all. These cases are all handled similarly with one Q-Twist or several Q-Twists where all but one of them are flipping of single edges.

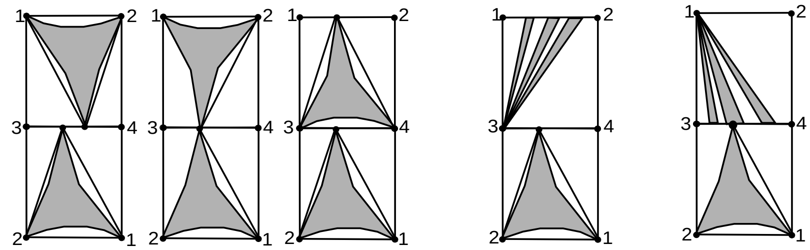

Figure 11.
Case 1.1.2: The lower quadrilateral is the interior of C_H.

Case 1.1.2.2 Let $N = \mathcal{B}' \setminus V$. The apex of N is either on the same branch of H as the apex of V or not. In the latter case, the configuration for V and N is the fourth one shown in Figure 11. (Again we assume that there is a V_{int}-type bridge in V. The reader can check the cases where there is not.) We can now go from σ_1 to σ_2 by a single Q-Twist hinged on the non-apex attachments of V and latched at the apices of V and N. No fixed bridges can block this.

In the former case, the configuration for V and N is last shown in Figure 11. Let N_r be the bridges of N whose extreme attachments are both at or to the right (relative to the figure) of the apex of V. We now go from σ_1 to σ_2 by first performing Q-Twists to individually reembed each bridge in N_r. Second, for the remaining bridges of $N \setminus N_r$, there can be no fixed H-bridges with attachments on the path connecting the extreme attachments of $N \setminus N_r$. Hence we can now perform a Q-Twist hinged on the extreme attachments of $N \setminus N_r$ and V and latched on the apex vertices of N and V. No fixed bridges can block these Q-Twists.

Case 1.1.3 Here $\mathcal{B}'$ consists of one or two end fans. We assume that there are two as the details for just one are contained in the proof for two. Denote these two fans by N_1 and N_2. We split this case into the following subcases: in Case 1.1.3.1, both fans share the same apex, say a on $\gamma_{i,i+1}$; in Case 1.1.3.2, the apices of the fans are the distinct endpoints of $\gamma_{i,i+1}$; in Case 1.1.3.3, the apices of the two fans are on different branches.

Case 1.1.3.1 The fan N_j is contained in a possibly larger fan $\overline{N}_j$ with apex a which might include reembeddable but fixed bridges. Such bridges are shown in black in Figure 12. Consider two H-bridges $B_1 \in \overline{N}_1$ and $B_2 \in \overline{N}_2$ whose paths between their extreme feet on $\gamma_{i+n,i+1+n}$ overlap in at least an edge. It must be that B_1 and B_2 are both fixed or both reembedded. Therefore, the path $\gamma_{i+n,i+1+n}$ decomposes into subpaths $P_1, \dots, P_k$ (some possibly of length zero) with the following properties: first, $P_m \cap P_{m+1}$ is a single vertex for each $1 \leq m \leq k-1$; second, each bridge in $\overline{N}_1 \cup \overline{N}_2$ has all of its attachments (aside from a) on some in P_l; third, each I-type bridge in $\overline{N}_1 \cup \overline{N}_2$ can then be assigned to a single P_l containing its non-apex attachment such that all of the bridges which are assigned to P_l are either all reembedded or all fixed; and fourth, if all bridges assigned to P_l are fixed, then all bridges assigned to P_{l+1} are all reembedded. Thus we can take σ_1 to σ_2 by a sequence of $\lceil \frac{k}{2} \rceil$ degenerate Q-Twists, hinged at endpoints of the P_l's and latched at a.

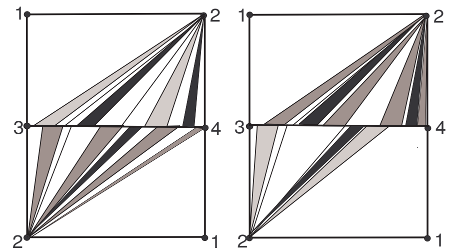

Figure 12.
Case 1.1.3.1: Fixed bridges are shown in black.

Case 1.1.3.2 Let a_t be the apex of N_t. Without loss of generality, say N_1 is interior to C_H in σ_1. Figure 13 shows N_1 and N_2 in σ_1 and σ_2 where the lower quadrilateral is interior to C_H. Given $\{j,k\} = \{1,2\}$, it may be the case that there are bridges in N_j that have no attachment on $\gamma_{i+n,i+1+n}$ that is to the left (relative to the figure) of the rightmost attachment of N_k. If so, then assume without loss of generality that $j = 1$ such as what is shown in Figure 13. Let $N_1' \subseteq N_1$ be the collection of these bridges. Each individual bridge in N_1' may be reembedded using a degenerate Q-Twist to obtain embedding σ_1', shown Figure 13. (No fixed bridges can block these Q-Twists; however, we cannot reembed all of the bridges by a single Q-Twist as there may be fixed bridges with attachments between $N_1 \setminus N_1'$ and N_1' that would block such a Q-Twist such as that shown in Figure 13.) Now given $\{x,y\} = \{1,2\}$, it may be the case that there are bridges in N_x that have no attachment on $\gamma_{i+n,i+1+n}$ that is to the right of the leftmost attachment of N_y. We reembed all of the bridges in $N_2 \cup (N_1 \setminus N_1')$ save these latter ones mentioned by a single Q-Twist (no fixed bridge may block this Q-Twist) to obtain embedding σ_2' (see Figure 13). Finally we go from σ_2' to σ_2 by performing individual Q-Twists on each of the remaining bridges of $\mathcal{B}'$.

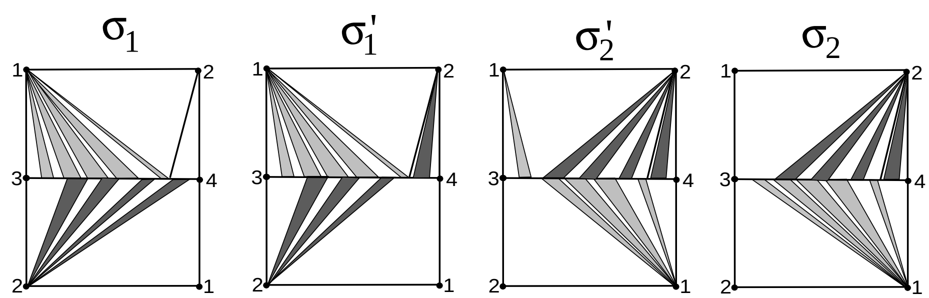

Figure 13.
Case 1.1.3.2

Case 1.1.3.3 Let a_t be the apex of N_t for each $t \in \{1,2\}$. Because a_1 and a_2 are on different branches of H, the bridges of N_1 overlap the bridges of N_2 in one of F_i or C_H and not in the other. Call the face where they overlap the *overlap face*. Without loss of generality, say N_1 is embedded in the overlap face in σ_1. In Figure 14 the overlap face is the lower square region. We may now reembed each bridge of N_1 individually by a Q-Twist to obtain σ_1' as in Figure 14. We then reembed each bridge of N_2 individually by a Q-Twist to obtain σ_2.

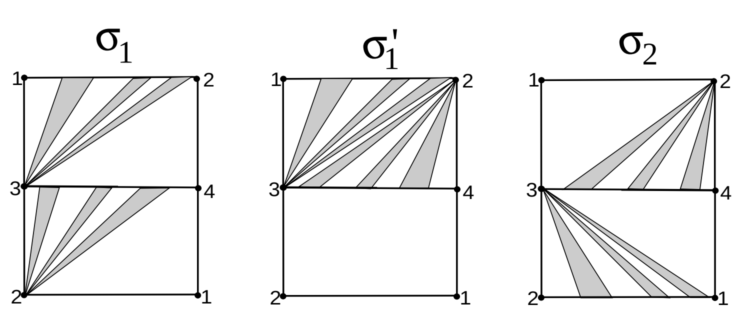

Figure 14.
Case 1.1.3.3

Case 1.2 Suppose that all reembedded bridges belong to distinct faces F_i and F_j. In Case 1.2.1, we assume that F_i and F_j do not share a common boundary edge, while in Case 1.2.2, we assume that $j = i + 1$.
Case 1.2.1 In this case any reembedded bridge belonging to F_i overlaps on C_H any reembedded bridge belonging to F_j. Hence there is an intermediate embedding σ_1' with all of the reembedded bridges exterior to C_H. We go from σ_1 to σ_1' as in Case 1.1 and from σ_1' to σ_2 also as in Case 1.1.
Case 1.2.2 Let $\mathcal{B}_i'$ and $\mathcal{B}_{i+1}'$ be the collections of reembedded H-bridges belonging to F_i and F_{i+1}, respectively. Let $B_i \in \mathcal{B}_i'$ and $B_{i+1} \in \mathcal{B}_{i+1}'$. Then unless B_i and B_{i+1} are both V_{end}- or I-type bridges with the same apex vertex, B_i and B_{i+1} will overlap on C_H. In the case that there does not exist B_i and B_{i+1} that are non-overlapping on C_H, we finish as in Case 1.2.1. If such an overlapping pair does exist, we can assume without loss of generality that branch vertex $i + 1$ is the common apex. So let $\mathcal{N}_i$ be the collection of reembedded V_{end}- and I-type bridges with apex vertex $i + 1$ belonging to F_i and let $\mathcal{N}_{i+1}$ be the collection of reembedded V_{end}- and I-type bridges with apex vertex $i + 1$ belonging to F_{i+1}. Hence any overlapping pair B_i and B_{i+1} are now in $\mathcal{N}_i$ and $\mathcal{N}_{i+1}$, respectively.

In Case 1.2.2.1, we assume that there are bridges of $\mathcal{N}_i$ in both the exterior and interior of C_H in σ_1. In Case 1.2.2.2, $\mathcal{N}_i$ has bridges only in the interior of C_H in σ_1 and $\mathcal{N}_{i+1}$ does not have bridges in both the interior and exterior of C_H in σ_1.
Case 1.2.2.1 Without loss of generality we split this case into the following two subcases. In Case 1.2.2.1.1 assume that $\mathcal{B}_i' \setminus \mathcal{N}_i \neq \emptyset$ and in Case 1.2.2.1.2 that $\mathcal{B}_i' \setminus \mathcal{N}_i = \mathcal{B}_{i+1}' \setminus \mathcal{N}_{i+1} = \emptyset$.
Case 1.2.2.1.1 First, because $\mathcal{B}_{i+1}' \neq \emptyset$, $\mathcal{B}_i' \setminus \mathcal{N}_i$ cannot have bridges in both the interior and exterior of C_H in σ_1. Without loss of generality, assume that the bridges of $\mathcal{B}_i' \setminus \mathcal{N}_i$ are interior to C_H in σ_1. Second, because $\mathcal{B}_i' \setminus \mathcal{N}_i$ has its bridges in the interior of C_H in σ_1, $\mathcal{B}_{i+1}'$ has no bridges interior to C_H in σ_1. Thus the bridges of $\mathcal{B}_{i+1}'$ form a fan exterior to C_H in σ_1; furthermore, the apex of this fan must be at branch vertex $i + 1$ in order to avoid overlapping with the bridges of $\mathcal{N}_i$ that are interior to C_H in σ_2. Third, the bridges of $\mathcal{B}_i'$ inside C_H must form a fan with apex on branch $\gamma_{n+i,n+i+1}$. In Figure 15 we show $\mathcal{B}_i'$ and $\mathcal{B}_{i+1}'$ in σ_1 and σ_2, respectively.

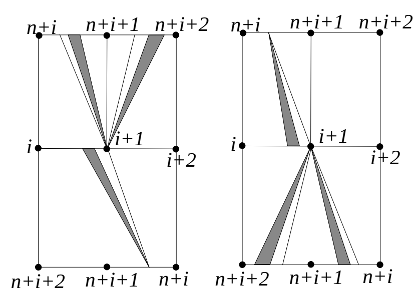

Figure 15. Case 1.2.2.1.1

Thus there is an intermediate embedding σ_1' with all of the bridges of $\mathcal{B}_{i+1}'$ exterior to C_H and all other H-bridges as in σ_2. We now go from σ_1 to σ_1' and from σ_1' to σ_2 as in Case 1.1.
Case 1.2.2.1.2 We complete this case in a manner very similar to Case 1.1.3.1 (see Figure 12).
Case 1.2.2.2 In this case, the bridges of $\mathcal{N}_i$ are all interior to C_H in σ_1 and so any bridge in $\mathcal{B}_{i+1}' \setminus \mathcal{N}_{i+1}$ is exterior to C_H in σ_1. In Case 1.2.2.2.1, $\mathcal{B}_i' \setminus \mathcal{N}_i \neq \emptyset$ and has bridges interior to C_H in σ_1. In Case 1.2.2.2.2, $\mathcal{B}_i' \setminus \mathcal{N}_i \neq \emptyset$ and has no bridges interior to C_H in σ_1. In while in Case 1.2.2.2.3, $\mathcal{B}_i' \setminus \mathcal{N}_i = \emptyset$.
Case 1.2.2.2.1 Here the bridges of $\mathcal{B}_{i+1}'$ are exterior to C_H and form a fan with apex either at branch vertex $i + 1$ or on $\gamma_{n+i+1,n+i+2}$ and all bridges of $\mathcal{B}_i$ are interior to C_H in σ_1. See the two configurations on the left of Figure 16. Thus there is σ_1' in which all bridges of $\mathcal{B}_i' \cup \mathcal{B}_{i+1}'$ are exterior to C_H and all other H-bridges are as in σ_1. We go from σ_1 to σ_1' and from σ_1' to σ_2 as in Case 1.1.

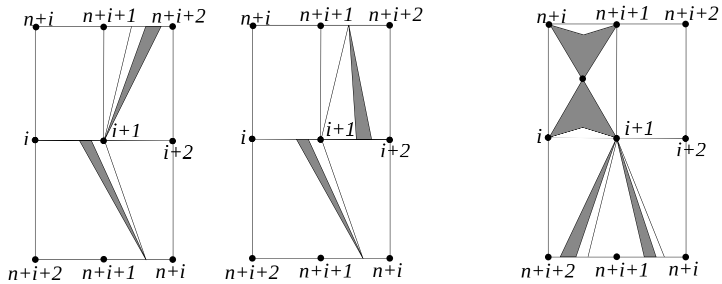

Figure 16.
The two possibilities for Case 1.2.2.2.1 are on the left and the configuration for Case 1.2.2.2.2 is shown on the right.

Case 1.2.2.2.2 In this case there are bridges of $\mathcal{B}'_i$ both interior and exterior to C_H in σ_1 while all of the bridges of $\mathcal{B}'_{i+1}$ are interior to C_H in σ_1. (See the configuration on the right of Figure 16.) There is an intermediate embedding σ'_1 in which all of the bridges of $\mathcal{B}'_{i+1}$ are exterior to C_H and all other H-bridges are as in σ_1. We go from σ_1 to σ'_1 and from σ'_1 to σ_2 as in Case 1.1.
Case 1.2.2.2.3 Here $\mathcal{B}'_i = \mathcal{N}_i$ and all of these bridges are interior to C_H in σ_1. There is an intermediate embedding σ'_1 in which all of the bridges of $\mathcal{B}'_i$ are exterior to C_H and all other H-bridges are as in σ_1. We go from σ_1 to σ'_1 and from σ'_1 to σ_2 as in Case 1.1.
Case 1.3 Suppose that all reembedded bridges belong to three distinct F_i's. It cannot be that the three F_i's are pairwise nonadjacent because reembedded bridges belonging to nonadjacent F_i's are overlapping on C_H. Without loss of generality, we can assume that these F_i's are F_1, F_2, and F_j, for j in $\{3, n-1\}$.

Since any reembedded bridge belonging to F_j overlaps on C_H any reembedded bridge belonging to F_1, we can assume that the reembedded bridges belonging to F_1 are exterior to C_H and those belonging to F_j are interior to C_H in σ_1. Therefore there exists an intermediate embedding σ'_1 with all the reembedded bridges belonging to F_j exterior to C_H and all other reembedded bridges are as in σ_1. So we go from σ_1 to σ'_1 as in Case 1.1 and as a second step from σ'_1 to σ_2 as in Case 1.2.
Case 1.4 Suppose that all reembedded bridges belong to at least four distinct F_i's. Here each such F_i has reembedded bridges which are overlapping with a reembedded bridge belonging to some F_k with $k \neq i$. Thus, the reembedded bridges belonging to F_i are all exterior to or all interior to C_H in σ_1. There is an intermediate embedding σ'_1 in which all reembedded bridges are exterior to C_H. We can go from σ_1 to σ'_1 and then from σ'_1 to σ_2 as in Cases 1.1, 1.2, and 1.3.
Case 2 Suppose $\sigma_1|_H = \nu_0$ and $\sigma_2|_H = \nu_1$ (See Figure 17).

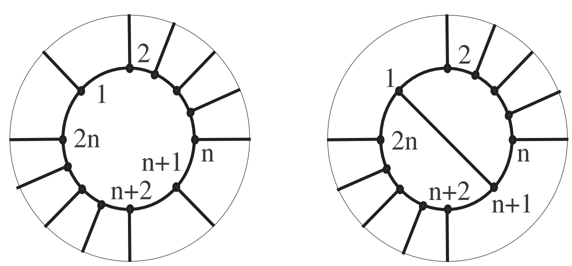

Figure 17.
Embeddings of H in Case 2

There are three types of H-bridges that are reembeddable. First, any H-bridge B with attachments in the interior of $\gamma_{1,n+1}$ must be reembedded and so all of the other attachments of B are on exactly one of $\gamma_{1,2}$, $\gamma_{1,2n}$, $\gamma_{n,n+1}$, $\gamma_{n+1,n+2}$. Let B_2, B_{2n}, B_n, and B_{n+2}, respectively, be the collections of these bridges with attachments on the interior $\gamma_{1,n+1}$. Second, H-bridges that have all attachments on $\gamma_{2n,1} \cup \gamma_{1,2}$ or all attachments on $\gamma_{n,n+1} \cup \gamma_{n+1,n+2}$. These types of bridges must be reembedded and we denote the collections of these bridges by B_1 and B_{n+1}. Let $\mathcal{B}$ be the collection of all of these bridges in B_z

(for $z \in \{1, 2, n, n+1, n+2, 2n\}$) along with $\gamma_{1,n+1}$. Third, bridges with attachments on both paths $\gamma_{2n,1} \cup \gamma_{1,2}$ and $\gamma_{n,n+1} \cup \gamma_{n+1,n+2}$. Let $\mathcal{A}$ denote the collection of these types of bridges.

Recall that for any collection of reembedded H-bridges that are all interior or all exterior to C_H, there must be a cut vertex c which prevents two vertex-disjoint C_H-paths in the collection because any two such paths would cross if reembedded.

Let α_1 be the subpath of $\gamma_{2n,1} \cup \gamma_{1,2}$ between the extreme attachments of $\mathcal{B}$. Let β_1 be the similarly defined subpath of $\gamma_{n+2,n+1} \cup \gamma_{n+1,n}$. Now let $H_1 = H \cup (\bigcup \mathcal{B})$ [††] and we can perform a Q-Twist on $\sigma_2|_{H_1}$ that is hinged on the endpoints of α_1 and β_1 in $\sigma_2|_{H_1}$ and latched at some vertex $c_1 \in \gamma_{1,n+1}$. If this Q-Twist can be extended to all of G in σ_2, then we obtain an embedding σ_3 for which $\sigma_1|_H = \sigma_3|_H = \nu_0$ and then we can go from σ_3 to σ_1 by a sequence of Q-Twists as in Case 1. If we cannot extend this Q-Twist to all of G, then there are H-bridges in $\mathcal{A}$ exterior to C_H in σ_2 that block this Q-Twist. Let $\mathcal{A}_1$ be the collection of these H-bridges in $\mathcal{A}$. Let $H_2 = H_1 \cup (\bigcup \mathcal{A}_1)$, α_2 extends α_1 to the extreme attachments of $\mathcal{A}_1$ on $\gamma_{2n,1} \cup \gamma_{1,2}$, and β_2 extends β_1 similarly. We can now perform a Q-Twist on $\sigma_2|_{H_2}$ that is hinged on the endpoints of α_2 and β_2 in $\sigma_2|_{H_2}$ and latched at vertices c_2^a and c_2^b. If this Q-Twist can be extended to all of G in σ_2, then we obtain an embedding σ_3 and then go to σ_1 as in Case 1. If not, then there are H-bridges interior to C_H in σ_2 that block this Q-Twist. Let $\mathcal{A}_2$ be the collection of such H-bridges. Let $H_3 = H_2 \cup (\bigcup \mathcal{A}_2)$, α_3 extends α_2 to the extreme attachments of $\mathcal{A}_2$ on $\gamma_{2n,1} \cup \gamma_{1,2}$, and β_3 extends β_2 similarly. Define a Q-Twist on $\sigma_2|_{H_3}$ that is hinged on the endpoints of α_3 and β_3 and latched at c_3^a and c_3^b. If we can extend this Q-Twist to all of G in σ_2, then we are done. If not, then define $\mathcal{A}_3$ and iterate this process again. Of course, this process must end as G is finite.

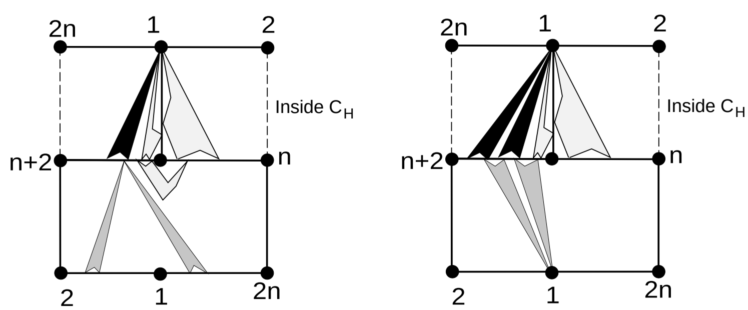

Figure 18.
Two illustrations of the iterative process: the light grey bridges are $\mathcal{B}$, the dark grey bridges are in $\mathcal{A}_1, \mathcal{A}_3, \ldots$, and the black bridges are in $\mathcal{A}_2, \mathcal{A}_4, \ldots$.

Case 3 Suppose $\sigma_1|_H = \sigma_2|_H = \nu_1$. Consider the faces of H as labeled in Figure 19.

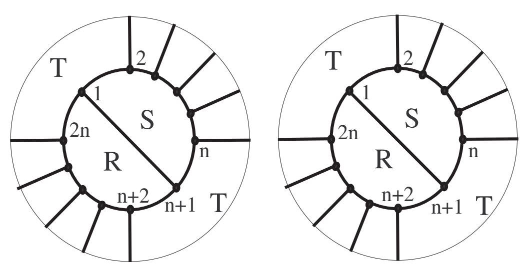

Figure 19.
Embeddings of H in Case 3

The only types of reembeddable bridges are those with all attachments on $\gamma_{1,2} \cup \gamma_{n,n+1}$ or all attachments on $\gamma_{2n,1} \cup \gamma_{n+1,n+2}$. Let $\mathcal{S}$ and $\mathcal{R}$, respectively, be the collections of such bridges that are actually reembedded. If there is some reembedded bridge $B \in \mathcal{R} \cup \mathcal{S}$ which contains an H-path γ with both endpoints off of $\{2, n, n+2, 2n\}$, then if we replace $\gamma_{1,n+1}$ in H with γ, then we obtain a new subdivision

[††] When $\mathcal{S}$ is a set of sets, we use $\bigcup S$ to denote the union of the sets in $\mathcal{S}$.

H' of V_{2n} in which $\{\sigma_1|_{H'}, \sigma_2|_{H'}\} = \{\nu_0, \nu_1\}$. It may be that H' has local H'-bridges. We may now reapply Lemma 6.2.1 of [9] to H' to get H'' with no local bridges and the same branch vertices as H'. Furthermore, in the proof of Lemma 6.2.1 of [9] we find that a branch β'' of H'' corresponding to β' of H' is contained within the union of β' along with the local H'-bridges of β'. Let G' be the subgraph of G consisting of H' along with its local H'-bridge. In the embeddings $\sigma_1|_{G'}$ and $\sigma_2|_{G'}$, each of branch β' of H' along with the local bridges of β' are embedded within some closed disk $D_{\beta'}$. These closed disks for the branches of H' may be chosen so that any pair intersects only at common branch vertices. As such, $\sigma_1|_{H'} = \sigma_1|_{H''}$ and $\sigma_2|_{H'} = \sigma_2|_{H''}$. We now can go from σ_1 to σ_2 as in Case 1 using H''.

So now the reembedded H-bridges of $\mathcal{R} \cup \mathcal{S}$ form one or two fan structures with apices in $\{2, n, n+2, 2n\}$; either two fans for $\mathcal{R}$, two fans for $\mathcal{S}$ or one fan for each of $\mathcal{R}$ and $\mathcal{S}$. So now all of the reembedding of G is happening within a 2-region Möbius strip with regions $\mathsf{R} \cup \mathsf{S}$ and T as in Case 1.1.3. The only difference between our current situation and Case 1.1.3 is that $\gamma_{1,n+1}$ cuts one region of the strip and that there may be fixed H-bridges attached to $\gamma_{1,n+1}$. However, $\gamma_{1,n+1}$ and any of these fixed bridges cannot interfere with the reembedding of the fans as described in Case 1.1.3. Thus we may take σ_1 to σ_2 as in Case 1.1.3.

Case 4 Suppose $\sigma_1|_H = \nu_1$ and $\sigma_2|_H = \nu_2$ (see Figure 20).

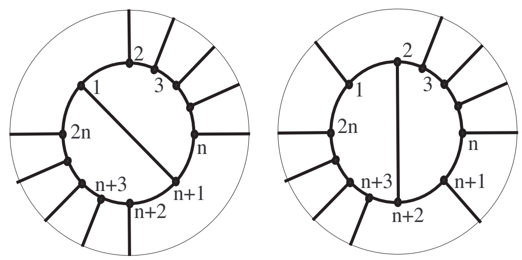

Figure 20.

Embeddings of H for Case 4.

Partition the reembedded bridges into two sets $\mathcal{B}_{in}$ and $\mathcal{B}_{out}$ for those that are interior and exterior, respectively, to C_H in σ_1. Note that any H-bridge with an attachment on the interior of $\gamma_{1,n+1}$ is in $\mathcal{B}_{in}$ and any H-bridge with an attachment in the interior of $\gamma_{2,n+2}$ is in $\mathcal{B}_{out}$. Suppose that B is an H-bridge with an attachment in the interior of $\gamma_{1,n+1}$. Then all of the other attachments of B are on exactly one of $\gamma_{1,2n}$, $\gamma_{1,2} \cup \gamma_{2,3}$, $\gamma_{n,n+1}$, $\gamma_{n+1,n+2} \cup \gamma_{n+2,n+3}$. Let $B_{1,2n}$, $B_{1,2,3}$, $B_{n,n+1}$, $B_{n+1,n+2,n+3}$, respectively, be the collections of these bridges with attachments on $\gamma_{1,n+1}$. Similarly bridges with attachments in the interior of $\gamma_{2,n+2}$ partition into the following four classes: $B_{2,1,2n}$, $B_{2,3}$, $B_{n+2,n+1,n}$, $B_{n+2,n+3}$.

Let B'_1 be the collection H-bridges with all attachments on $\gamma_{2n,1} \cup \gamma_{1,2}$. Let B'_{n+1} be the collection of H-bridges with all attachments $\gamma_{n,n+1} \cup \gamma_{n+1,n+2}$. Note $B'_1 \cup B'_{n+1} \subseteq \mathcal{B}_{out}$. Similarly, we define B'_2 and B'_{n+2}, where $B'_2 \cup B'_{n+2} \subseteq \mathcal{B}_{in}$.

Let $\mathcal{B}_1 = B_{1,2n} \cup B_{1,2,3} \cup B_{n,n+1} \cup B_{n+1,n+2,n+3} \cup B'_1 \cup B'_{n+1} \cup \gamma_{1,n+1}$ and $\mathcal{B}_2 = B_{2,1,2n} \cup B_{2,3} \cup B_{n+2,n+1,n} \cup B_{n+2,n+3} \cup B'_2 \cup B'_{n+2} \cup \gamma_{2,n+2}$. Now $\mathcal{B}_1 \cup \mathcal{B}_2 \subseteq \mathcal{B}_{in} \cup \mathcal{B}_{out} \cup \{\gamma_{1,n+1}, \gamma_{2,n+2}\}$ with equality being possible. Let $\mathcal{F}_{out} = \mathcal{B}_{out} \setminus (\mathcal{B}_1 \cup \mathcal{B}_2)$ and $\mathcal{F}_{in} = \mathcal{B}_{in} \setminus (\mathcal{B}_1 \cup \mathcal{B}_2)$. Consider some $D \in \mathcal{F}_{in}$. The bridge D must have attachments on both of $\alpha = \gamma_{2n,1} \cup \gamma_{1,2} \cup \gamma_{2,3}$ and $\beta = \gamma_{n,n+1} \cup \gamma_{n+1,n+2} \cup \gamma_{n+2,n+3}$ and have all of its attachments on α and β. Furthermore, D cannot contain a path from α to β that is vertex disjoint from $\gamma_{1,n+1}$. Thus either the only attachment of D on α is branch vertex 1 or the only attachment of D on β is branch vertex $n+1$. Additionally, there cannot be $D_1 \in \mathcal{F}_{in}$ whose only attachment on α is vertex 1 and $D_2 \in \mathcal{F}_{in}$ whose only attachment on β is vertex $n+1$ because two such bridges would contain two vertex-disjoint paths from α to β. So without loss of generality we may assume that $\mathcal{F}_{in} = \emptyset$ or each $D \in \mathcal{F}_{in}$ has vertex 1 as its only attachment on α and all other attachments on β. In a similar fashion we get that either $\mathcal{F}_{out} = \emptyset$, each $D \in \mathcal{F}_{out}$ has vertex 2 as its only attachment on α, or each $D \in \mathcal{F}_{out}$ has vertex $n+2$ as its only attachment on β. We can also assume that $\mathcal{F}_{out} \neq \emptyset$ when $\mathcal{F}_{in} \neq \emptyset$.

If there is an embedding σ_3 of G in which $\sigma_3|_H = \nu_0$, then we can go from σ_1 to σ_3 and from σ_3 to σ_2 as in Case 2. So suppose that there is no such "intermediate" embedding σ_3. We now split the remainder of this case into the following five subcases: in Case 4.1 $\mathcal{F}_{in} = \mathcal{F}_{out} = \emptyset$, in Case 4.2 $\mathcal{F}_{in} = \emptyset$ and every $D \in \mathcal{F}_{out}$ has vertex 2 as its only attachment on α, in Case 4.3 $\mathcal{F}_{in} = \emptyset$ and every $D \in \mathcal{F}_{out}$ has vertex $n+2$ as its only attachment on β, in Case 4.4 $\mathcal{F}_{in} \neq \emptyset$ and every $D \in \mathcal{F}_{out}$ has vertex 2 as its only attachment on α, and in Case 4.5 $\mathcal{F}_{in} \neq \emptyset$ and every $D \in \mathcal{F}_{out}$ has vertex $n+2$ as its only attachment on β.

Case 4.1 Let α_1 be the subpath of α between the extremal attachments of $\mathcal{B}_1$ and let β_1 be the subpath of β between the extremal attachments of $\mathcal{B}_1$. Define α_2 and β_2 similarly for $\mathcal{B}_2$. Since the intermediate embedding σ_3 from the previous paragraph does not exist, it must be that either one of the α's has an endpoint in the interior of the other or one of the β's has an endpoint in the interior of the other. On the left in Figure 21 we show such a configuration for σ_1 in which the β's overlap but α's do not overlap. Now we define a Q-Twist on σ_1 that is hinged on the endpoints of $\alpha_1 \cup \alpha_2$ on α and $\beta_1 \cup \beta_2$ in β and latched at vertices in the interior of $\gamma_{1,n+1}$ and $\gamma_{2,n+2}$ to obtain a new embedding of G. One can check that no fixed bridges are possible with attachments on α and β that would block this Q-Twist. Since $\mathcal{F}_{in} \cup \mathcal{F}_{out} = \emptyset$, the resulting embedding is σ_2, as required.

Figure 21.

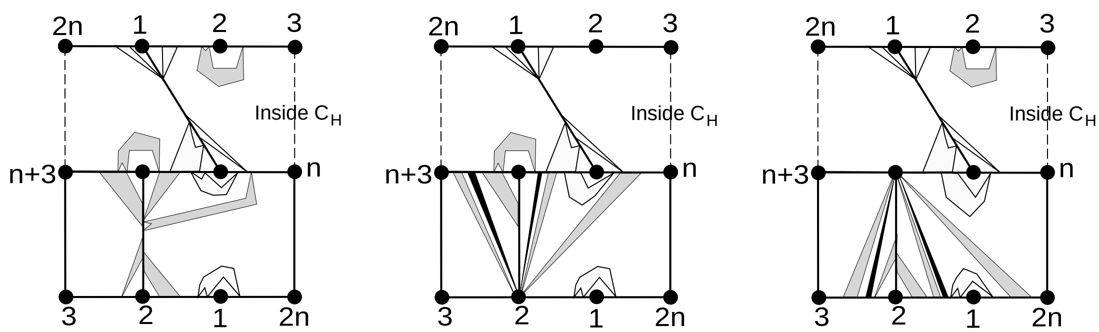

Bridge configurations for Case 4.

Case 4.2 In this case $B_{2,1,2n} = B_{2,3} = \emptyset$ because, otherwise, given a bridge in $B \in B_{2,1,2n} = B_{2,3}$ and a bridge $D \in \mathcal{F}_{out}$, we have that $B \cup \gamma_{2,n+2} \cup D$ would contain two vertex-disjoint C_H-paths. Let α_1, α_2, and β_1 be as defined in Case 4.1 and let β_2 be the subpath of β connecting the extremal attachments of bridges in $\mathcal{F}_{out} \cup \mathcal{B}_2$. Again, because the intermediate embedding σ_3 does not exist, either one of the α's has an endpoint in the interior of the other or one of the β's has an endpoint in the interior of the other. The second configuration shown in Figure 21 shows an overlap of the β's but not the α's. Now we can define a Q-Twist on σ_1 that is hinged on the endpoints of $\alpha_1 \cup \alpha_2$ in α and $\beta_1 \cup \beta_2$ in β and latched at vertex 2 and some other vertex in the interior of $\gamma_{1,n+1}$ to obtain a new embedding σ_4 of G. One can check that there are no fixed bridges with attachments on α (aside from vertex 2) that block this Q-Twist; furthermore, any fixed bridge with an attachment on β must be part of the fan-type structure with apex at vertex 2 analogous to the black bridges shown in the second configuration of Figure 21. Such fixed bridges are reembedded by this Q-Twist from σ_1 to σ_4. The resulting embedding σ_4 has $\sigma_4|_H = \nu_2$. We can now go from σ_4 to σ_2 as in Case 3.

Case 4.3 Analogous to Case 4.2 with $B_{n+2,n+1,n} = B_{n+2,n+3} = \emptyset$ and the Q-Twist defined on σ_1 having its latch at vertex $n+2$ rather than vertex 2. (See the rightmost configuration in Figure 21.)

Case 4.4 Recall that each $D \in \mathcal{F}_{in}$ has vertex 1 as its sole attachment on α and has all other attachments on β. Hence $B_{1,2n} = B_{1,2,3} = \emptyset$ as well as $B_{2,1,2n} = B_{2,3} = \emptyset$. Define the α_1 and α_2 as before, define β_1 as the subpath of β connecting the extremal attachments of bridges in $\mathcal{F}_{in} \cup \mathcal{B}_1$, and define β_2 as the subpath of β connecting the extremal attachments of bridges in $\mathcal{F}_{out} \cup \mathcal{B}_2$. Again, we must have that either one of the α's has an endpoint in the interior of the other or one of the β's has an endpoint in the interior of the other. The first configuration shown in Figure 22 shows an overlap of the β's but not the α's and the second configuration shows an overlap of the α's but not the β's. We can now define a Q-Twist on σ_1 hinged at the endpoints of $\alpha_1 \cup \alpha_2$ on α and $\beta_1 \cup \beta_2$ on β and latched at vertices 1 and 2 taking σ_1 to a new embedding σ_4. One can check that any fixed bridge with attachments on α and β must be part of one of the fan-type structures with apex at vertex 1 or 2 analogous to those shown in black in the first two configurations of Figure 22. These fixed bridges are included in this Q-Twist taking σ_1 to σ_4 with $\sigma_4|_H = \nu_2$. We can now go from σ_4 to σ_2 as in Case 3.

Figure 22.

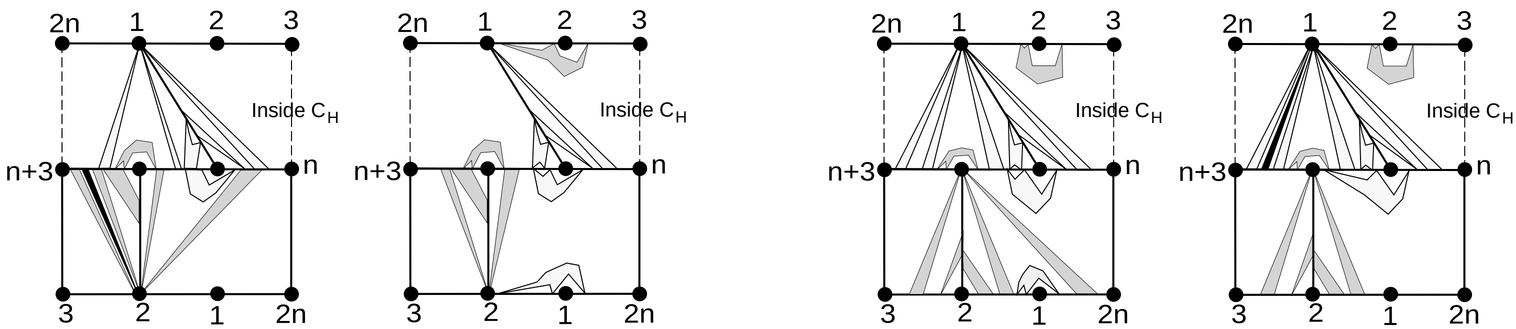

More bridge configurations for Case 4.

Case 4.5 Again, remember that each $D \in \mathcal{F}_{in}$ has vertex 1 as its sole attachment on α and has all other attachments on β. Hence $B_{1,2n} = B_{1,2,3} = B_{2,n+3} = B_{2,n+1,n} = \emptyset$. Define α_1 and β_2 as in Case 4.1, define α_2 to be the subpath of α connecting the extremal attachments of bridges in $\mathcal{B}_2 \cup \mathcal{F}_{out}$, and define β_1 to be the subpath of β connecting the extremal attachments of bridges in $\mathcal{B}_1 \cup \mathcal{F}_{in}$. Again we must have overlap of the α's or β's. The two configurations on the right in Figure 22 show two possibilities for such types of overlapping on α and/or β. Any fixed bridges with attachments on $\alpha \cup \beta$ must be part of the fan structures analogous to what is shown in black. Now we can define a Q-Twist on σ_1 hinged on the endpoints of $\alpha_1 \cup \alpha_2$ on α and the endpoints of $\beta_1 \cup \beta_2$ on β and latched at vertices 1 and $n+2$. This Q-Twist takes σ_1 to σ_4 with $\sigma_4|_H = \nu_2$. We can now go from σ_4 to σ_2 as in Case 3.

Case 5: Suppose $\sigma_1|_H = \nu_1$ and $\sigma_2|_H = \nu_j$ for $3 \leq j \leq n-1$. See Figure 23. In Case 5.1 say that $n \geq 5$ and in Case 5.2 say that $n = 4$.

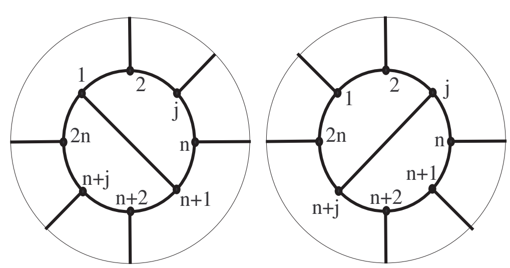

Figure 23.

Embeddings of H in Case 5.

Case 5.1 Since $n \geq 5$, there are only two types of reembeddable bridges. Following similar notation as we did in Case 4, the first type of reembeddable bridges partition into the following 12 sets: $B_{1,2}$, $B_{1,2n}$, B'_1, $B_{n+1,n}$, $B_{n+1,n+2}$, B'_{n+1} and $B_{j,j-1}$, $B_{j,j+1}$, B'_j, $B_{n+j,n+j-1}$, $B_{n+j,n+j+1}$, B'_{n+j}. Say that bridges in the first six sets *go along* with $\gamma_{1,n+1}$ and bridges from the second six sets go along with $\gamma_{j,n+j}$. The second type of reembeddable bridges partition into fans with apex vertices from $\{v_1, v_{n+1}\}$ or $\{v_j, v_{n+j}\}$. Say that bridges in fans with apex from the first set go along with $\gamma_{1,n+1}$ and bridges in fans with apex from the second set go along with $\gamma_{j,n+j}$.

So now in σ_1 all reembeddable bridges going along with $\gamma_{j,n+j}$ must be exterior to C_H except those in $B'_j \cup B'_{n+j}$ which must be interior to C_H. Similarly, in σ_2 all reembeddable bridges going along with $\gamma_{1,n+1}$ must be exterior to C_H except those in $B'_1 \cup B'_{n+1}$ which must be interior to C_H. Therefore there is an embedding σ_3 of G with all bridges going along with $\gamma_{j,n+j}$ and all bridges going along with $\gamma_{1,n+1}$ exterior to C_H except the bridges in $B'_1 \cup B'_{n+1} \cup B'_j \cup B'_{n+j}$ which are all interior to C_H. Note that $\sigma_3|_H = \nu_0$ and so we go from σ_1 to σ_3 by a sequence of Q-Twists as in Case 2 and we go from σ_3 to σ_2 by a sequence of Q-Twists as in Case 2.

Case 5.2 Here $n = 4$ and so $\sigma_1|_H = \nu_1$ and and $\sigma_2|_H = \nu_3$. See Figure 24 for a different rendering of these embeddings. Recall that C_H is the octagon with vertices $1, 2, 3, 4, 5, 6, 7, 8$ which is on the lower right in these figures.

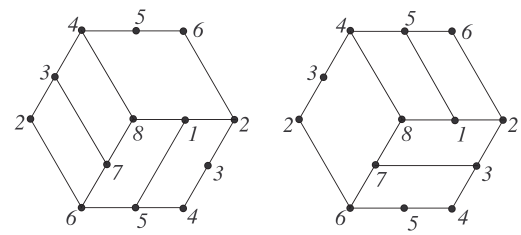

Figure 24.
A different rendering of the two embeddings of H in Case 5.2.

In this case, a fixed H-bridge need not have the same placement with respect to $\overline{H}$ in σ_1 and σ_2. This is because there may be H-bridges with all their attachments on $\gamma_{2,6} \cup \gamma_{4,8}$. So we do not use the terms fixed and reembedded in this case. (Again, these terms refer to an H-bridge B being inside or outside C_H and being outside C_H does not imply that B is embedded in a uniquely determined face of H, here in Case 5.2). We now partition the types of H-bridges that can exist in both embeddings of H into four different classes. First, a *singular bridge* is a single $(2,4)$-, $(4,6)$-, $(6,8)$-, or $(2,8)$-edge. For each of these singular bridges we say it has *corner vertex* 3, 5, 7, or 1, respectively. Second, a *corner bridge* is a bridge which has all attachments on two adjacent branches of H and is not a singular bridge. The branch vertex incident to both branches of a corner bridge is called the *corner vertex* of the bridge. Third, an *antipodal bridge* is a bridge that has all attachments on C_H that is not a corner bridge or a singular bridge. From Figure 24 we see that any antipodal bridge has all of its attachments on some $\gamma_{a,1+a} \cup \gamma_{4+a,5+a}$. Note that, by the maximality of V_8 among all V_{2n}-subdivisions in G, such a bridge cannot have attachments in the interiors of both $\gamma_{a,1+a}$ and $\gamma_{4+a,5+a}$ and that an antipodal bridge is exterior to C_H in both embeddings. Fourth, a *Petersen bridge* is a bridge which is not a corner bridge or singular bridge and either has an attachment in the interior of one of $\gamma_{2,6}$ and $\gamma_{4,8}$ or has all of its attachments on at least three vertices from $\{2, 4, 6, 8\}$. Note that a Petersen bridge is always exterior to C_H in both embeddings with all attachments on $\gamma_{2,6} \cup \gamma_{4,8}$. Further note that it is impossible to have both an antipodal bridge and a Petersen bridge, as both are exterior to C_H in both embeddings.

We split the remainder of this case into five subcases. In Case 5.2.1 we say that there is a Petersen bridge with attachments in the interiors of both $\gamma_{2,6}$ and $\gamma_{4,8}$. If there is no Petersen bridge having attachments in the interiors of both $\gamma_{2,6}$ and $\gamma_{4,8}$, then without loss of generality we can say that in Case 5.2.2 that there is a Petersen bridge with vertices of attachment 4, 8, and 9 where 9 is an interior vertex of $\gamma_{2,6}$, in Case 5.2.3 that there is a Petersen bridge attached at vertices 8 and 9 where 9 is an interior vertex of $\gamma_{2,6}$, in Case 5.2.4 that there is a Petersen bridge having three or four attachments all of which are from $\{2, 4, 6, 8\}$, and in Case 5.2.5 that there is no Petersen bridge. In Cases 5.2.1–5.2.4 let B denote the Petersen bridge identified.

Case 5.2.1 There is an H-path in B whose union with H forms a subdivision of the Petersen graph, call this subdivision P. Rechoose P so that it has no local bridges and the same branch vertices. There are two distinct labeled embeddings of P in the projective plane (a fact one can check or see [20]) and we claim that $\sigma_1|_P \neq \sigma_2|_P$. If we assume that $\sigma_1|_P = \sigma_2|_P$, then since any embedding of P has representativity 3, any P-bridge belongs to a unique face of P and so by 3-connectivity the embedding of a P-bridge in its face is unique and so $\sigma_1 = \sigma_2$, a contradiction.

Now, one can check that any P-bridge in G must have all of its attachments on two adjacent branches of P in order to belong to a face of both embeddings of P. Again we now have a unique corner vertex of P for any P-bridge. One can also check that for any (u, v)-branch of P, that the corner bridges for u and the corner bridges for v do not overlap along the (u, v)-branch or else they will cross in either σ_1 or σ_2. Thus we can go from σ_1 to σ_2 by a single P-Twist or a single degenerate P-Twist.

Case 5.2.2 Here $H \cup B$ again contains a Petersen graph subdivision and we finish as in Case 5.2.1.

Case 5.2.3 Here $H \cup B$ contains a subdivision of the 1-edge contraction of the Petersen graph, call it P', where $\sigma_1|_{P'}$ and $\sigma_2|_{P'}$ are as shown in Figure 25. Note that any P'-bridge is either an H-bridge or has attachments on the interior of the $(8, 9)$-branch of P'. Let $\mathcal{H}$ and $\mathcal{P}'$ be the collections of these two types of P'-bridges. The $(8, 9)$-branch may now be rechosen as in [9, 6.2.1] so that there are no local P'-bridges on the $(8, 9)$-branch and so since H has no local bridges, neither does P'.

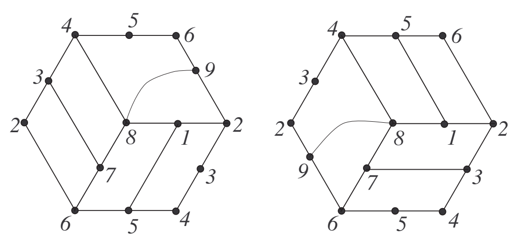

Figure 25.

Embeddings of H with an $(8, 9)$-branch attached.

Note that there can be no antipodal bridges in $\mathcal{H}$ and so any bridge in $\mathcal{H}$ is either a corner bridge or a singular bridge. Furthermore any corner bridge at vertex 8 must have all of its attachments on $\gamma_{1,8} \cup \gamma_{7,8}$. Any bridge in $\mathcal{P}'$ either has all attachments on branches incident with vertex 9 (i.e., one can think of these as corner bridges at corner vertex 9) or has all attachments on $\gamma_{4,8} \cup \gamma_{8,9}$. Thus there is a 1-edge decontraction G' of G at v_8 which extends the embeddings σ_1 and σ_2 to σ_1' and σ_2' analogous to what is shown in Figure 26. Note that a singular $(4, 8)$-bridge of G can be assigned to either vertex 8 or vertex $8'$ in G'. So now G' contains a subdivision of the Petersen graph and is 3-connected and so σ_1' and σ_2' are related by a single P-Twist as in Case 5.2.1. Thus σ_1 and σ_2 are related by this same P-Twist or a P-Twist obtained by a contraction of it.

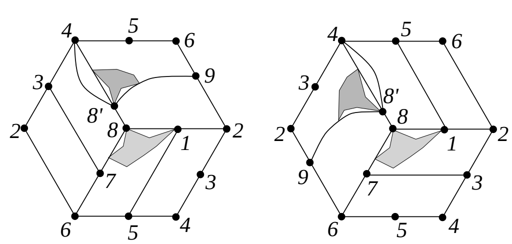

Figure 26.

Corner bridges for Case 5.2.3.

Case 5.2.4 Here $H \cup B$ contains a subdivision of the 1-edge contraction of the Petersen graph and so we finish as in Case 5.2.3.

Case 5.2.5 If there are no singular H-bridges, then since there are no Petersen bridges any H-bridge that is interior to C_H in both σ_1 and σ_2 or exterior to C_H in both σ_1 and σ_2 is fixed with respect to $\overline{H}$ and so we finish as in Case 5.1. So assume there are singular bridges. Either there is a singular bridge that is exterior to C_H in both embeddings or not. If not, then, similarly, any H-bridge that is interior to C_H in both σ_1 and σ_2 or exterior to C_H in both σ_1 and σ_2 is fixed with respect to $\overline{H}$ and so we finish as in Case 5.1. If so, then assume, without loss of generality, that the singular bridge is a $(6, 8)$-edge. Let H' be the union of H and the $(6, 8)$-edge. So $\sigma_1|_{H'}$ and $\sigma_2|_{H'}$ are as shown in Figure 27.

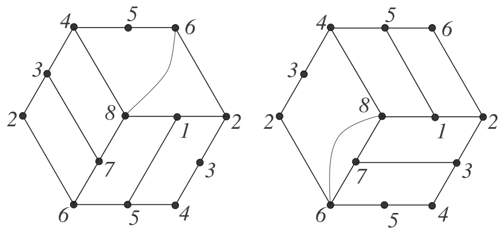

Figure 27.

Case 5.2.5.

Now in this case, we can perform a 1-edge decontraction of G at vertex 8 similar to Case 5.2.3 that extends the embeddings. Again we get that σ_1 and σ_2 are related by a single P-Twist.

5 Proof of Lemma 1.2 for V_8-free graphs

In this section, we will prove Lemma 1.2 in the case where G is V_8-free. Formally, we assume that G is 3-connected and V_8-free and has two embeddings σ_1 and σ_2 in the projective plane. We will show that these two embeddings are related by Q-Twists and P-Twists. We use Theorem 1.3 which characterizes internally 4-connected graphs with no V_8-minor. Hence we need to analyze the 3-separations of G to reduce to an internally 4-connected sub-structure in G. Two degenerate cases are where G is a 3-sum of two planar graphs (Section 5.2) and G is a 3-sum of two non-planar graphs (Section 5.3); these cases are both handled by a more general theorem presented in Section 5.1. The main analysis including the case analysis for the structures indicated in Theorem 1.3 comes in Section 5.4.

5.1 3-sums that split a $K_{3,4}$

We will refer to the vertices of $K_{3,4}$ by $1, 2, 3, 4$ and a, b, c as shown on the left in Figure 28. Suppose that $G = G_1 \oplus_3 G_2$ is 3-connected and contains a subgraph H that is subdivision of a 3-connected split of $K_{3,4}$ such that the two of the branch vertices of H corresponding to $1, 2, 3, 4$ (say 1 and 2) are contained in $V(G_1) \setminus V(G_2)$ and the other two (3 and 4) are contained in $V(G_2) \setminus V(G_1)$. In this case, we say that the 3-sum $G = G_1 \oplus_3 G_2$ *splits a* $K_{3,4}$ *by* H or just *splits a* $K_{3,4}$.

Since G is a projective-planar graph, H is a subdivision of one of the three graphs shown in Figure 28, call them $K_{3,4}$, S_1 and S_2. Note that if c is split in a similar fashion, then an excluded minor for the projective plane results. Note that the three vertices of the 3-separation splitting $K_{3,4}$ by H must occur along the (a, a')- and (b, b')-branches when H is a subdivision of S_1 or S_2.

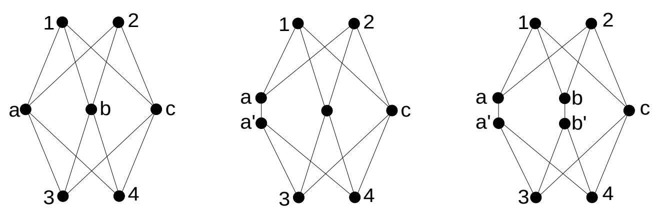

Figure 28.

The graphs $K_{3,4}$, S_1 and S_2.

Proposition 5.1. *If $G = G_1 \oplus_3 G_2$ is 3-connected, projective planar, and splits a $K_{3,4}$ by H, then any two embeddings σ_1 and σ_2 of G in the projective plane are related by a sequence of Q-Twists and P-Twists.*

Proof. Using [9, Lemma 6.2.1] we rechoose H so that it has the same branch vertices but no local bridges. Recall that this rechoosing procedure as described in [9, Lemma 6.2.1] takes each branch individually in union with its local bridges and finds the new branch from within this. Thus the new H is also split by $G = G_1 \oplus_3 G_2$.

In Case 1, say that H is a subdivision of $K_{3,4}$, in Case 2 say that H is a subdivision of S_1, and in Case 3, say that H is a subdivision of S_2.

Case 1 The H-bridges of G partition into three distinct types. Let S be the H-bridges that are single links on vertices a, b, c. For $i \in \{1, 2, 3, 4\}$ let B_i be the H-bridges whose attachments are all on the subdivided triad of H at vertex i and are not in S. For $(i, j) = (1, 2)$ or $(3, 4)$, let $B_{(i,j)}$ be the collection of H-bridges having attachments on both the subdivided triad at vertex i and at vertex j and are not in $S \cup B_1 \cup B_2 \cup B_3 \cup B_4$. Since a, b, c is a 3-separation there are no other H-bridges possible. In Case 1.1 say that $B_{(1,2)} = B_{(3,4)} = \emptyset$. In Case 1.2 say without loss of generality that $B_{(1,2)} = \emptyset$ and $B_{(3,4)} \neq \emptyset$. In Case 1.3 say that $B_{(1,2)}$ and $B_{(3,4)}$ are both nonempty.

Case 1.1 There are six embeddings of $K_{3,4}$ as shown in Figure 29. Excluding the H-bridges in S, the figure also depicts all of the possible embeddings of G as well. Note that 3-connectivity implies that each bridge in $B_1 \cup \cdots \cup B_4$ has only one possible placement for each embedding of H. Each arrow in the figure now represents a Q-Twist between the two embeddings at its ends with hinges and latches in a, b, c. For example, to change the embedding at the top of the figure to the adjacent one clockwise to it, use a Q-twist hinged at b, c and latched at a. Each edge in S has two possible placements for each embedding of H and these two placements are obtained by flipping the edges in S. Edges in S may also be included in a shaded region around vertices 1, 2, 3, or 4. Thus we can go between any two embeddings of G by a sequence of Q-Twists.

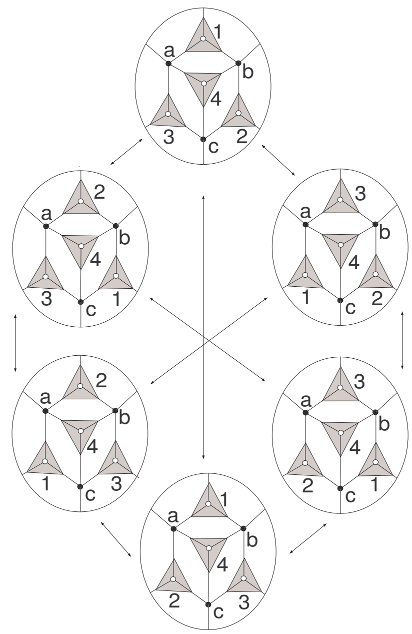

Figure 29.

The six embeddings of H along with bridges as indicated.

Case 1.2 We can assume without loss of generality that $\sigma_1|_H$ is the embedding of $K_{3,4}$ shown on the top of Figure 29. So now all H-bridges in $B_{(3,4)}$ must be embedded in the face F of $\sigma_1|_H$ defined by $a, 3, c, 4$. There are several possibilities for an H-bridge in $B_{(3,4)}$: a single $(3, 4)$-edge, an H-bridge with all attachments on the $(a, 3)$- and $(a, 4)$-branches but not a single $(3, 4)$-edge (call it an *a-corner*), an H-bridge with all attachments on the $(c, 3)$- and $(c, 4)$-branches but not a single $(3, 4)$-edge (call it an *c-corner*), and an H-bridge that is not of one of these three types. In the remainder of this paragraph we will show that the only H-bridge of this fourth type that we need consider is an H-bridge whose attachments are exactly $a, 3, c, 4$ (call it a *quad bridge*). So consider an H-bridge B of this fourth type. If B has attachments in the interiors of two antipodal branches of H on F, then one can find a V_8-subdivision in G and so our result holds by the result of Section 4. So if B does not have attachments in the interiors of two antipodal branches of H on F, then B must have at least three vertices of attachment. If B has an attachment in the interior of a branch of H on F (say the $(a, 4)$-branch), then there must be an attachment on $(a, 3)$-branch but not at a and on the $(c, 4)$-branch, not at 4. Such a bridge contains a subdivided triad on these three attachments and H union this triad contains a V_8-subdivision and so we get our result from Section 4. So B has no vertices of attachment on the interiors of the four branches of H on F. The only possibility is therefore a bridge whose vertices of attachment are $a, 3, c, 4$.

In Case 1.2.1, assume there is a quad bridge. In Case 1.2.2, there is no quad bridge, there is an a-corner, and no c-corner. In Case 1.2.3, there is no quad bridge and there are both a- and c-corners. In Case 1.2.4, there is only a single $(3, 4)$-edge.

Case 1.2.1 In this case there can be no $(3, 4)$-edge and a- or c-corner. The only possibilities for $\sigma_2|_H$ are the top and top-left embeddings of $K_{3,4}$-shown in Figure 29. So all possible embeddings of G are shown in Figure 30 up to flipping of (a, b)- and (b, c)-edges. Up to these flippings the embeddings are related by a single Q-Twist hinged at a, c and latched at b.

Figure 30.

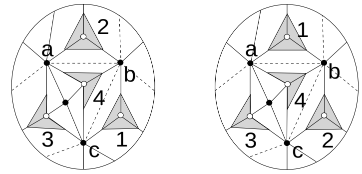

Case 1.2.1.

Case 1.2.2 If there is a $(3, 4)$-edge in G, then in this case we may treat it as an a-corner. There are only four possible embeddings of H that allow for an a-corner. They are shown on the left in Figure 31. Each bridge of $B_1 \cup \cdots \cup B_4 \cup A_{(3,4)}$ has only one possible placement for each embedding of H while the edges of S have one or two possible placements for each embedding of H (which are related by flipping). On the right of Figure 31 the the H-bridges in $B_3 \cup B_4$ may further restrict the possible embeddings of H when they overlap the H-bridges in the a-corner as shown. (In a symmetrical fashion, the overlap may restrict to the other two embeddings of H.) So without loss of generality all possible H-bridges and their placements in this case are shown in Figure 31.

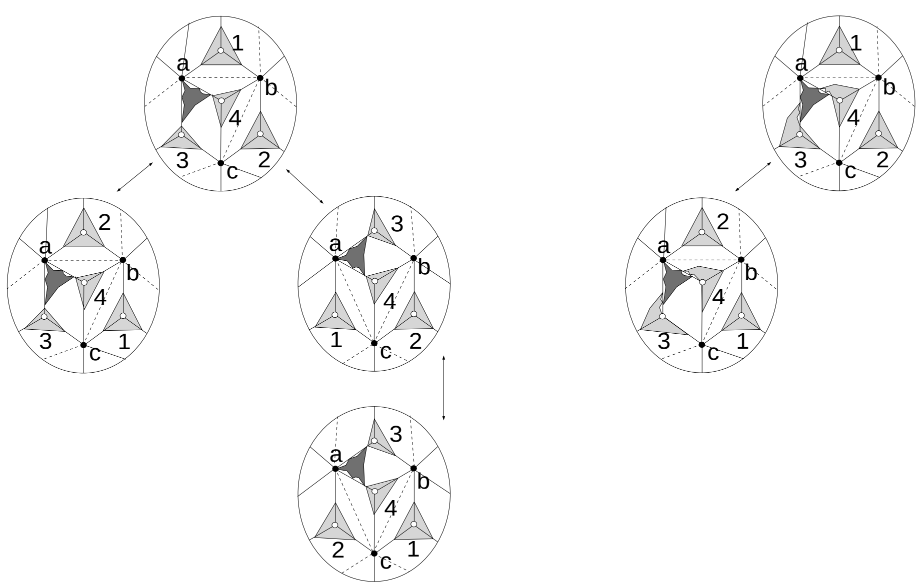

Figure 31.

Case 1.2.2.

The right-hand grouping of embeddings in Figure 31 are related by a Q-Twist hinged on a, c and latched at b and by flipping of edges in S. So now consider the left-hand grouping of embeddings. The top embedding and the one to its left (with any placement of the bridges in S) are related by a Q-Twist hinged at a, c and latched at b. Similarly, the bottom embedding and the one directly above are related by a Q-Twist hinged at a, b and latched at c. The top embedding and the one to its right (with the bridges in S flipped out) are related by a Q-Twist hinged at b, c, a, a_3 and latched at a, a_4 (where a_i is a vertex separating the a-corner from the B_i bridges on the (a, i)-branch). So aside from flipping edges in S, any two embeddings of G are related by Q-Twists.

Case 1.2.3 If there is a $(3, 4)$-edge in G, then in this case we may treat it as either an a- or c-corner. There are only two possible embeddings of H that allow for both a- and c-corners. They are shown in Figure 32. Each bridge of $B_1 \cup \cdots \cup B_4 \cup A_{(3,4)}$ has only one possible placement for each embedding of H (with possible overlap with a- and c-corners as in Case 1.2.2) while the edges of S have two possible placements for each embedding of H (which are related by flipping). All possible H-bridges and their placements in this case are thus shown in Figure 32. These embeddings are related by a Q-Twist hinged at a, c and latched at b and flipping of edges in S.

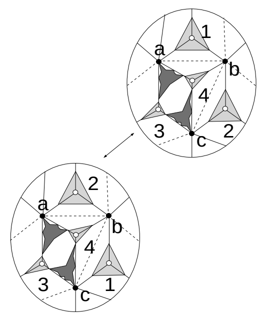

Figure 32.

Case 1.2.3.

Case 1.2.4 Here $B_{(3,4)}$ contains only the single $(3, 4)$-edge. If $B_3 = B_4 = \emptyset$, then the possible embeddings of G are shown on the left of Figure 33 up to flipping of single-edge bridges in S. Recall that $\sigma_1|_H$ is the top embedding. The double arrows again represent relations between the embeddings by Q-Twists. The arrows between pairs of embeddings in which the $(3, 4)$-edges are parallel are related by a Q-Twist hinged at two vertices from $\{a, b, c\}$ and latched at the third. The vertical arrow on the left represents a Q-Twist hinged at $a, 3, b, c$ and latched at $c, 4$ (with appropriate placement of the edges from S). The arrow at the top right represents a Q-Twist hinged at $a, b, 3, c$ and latched at $a, 4$ (with appropriate placement of the edges from S).

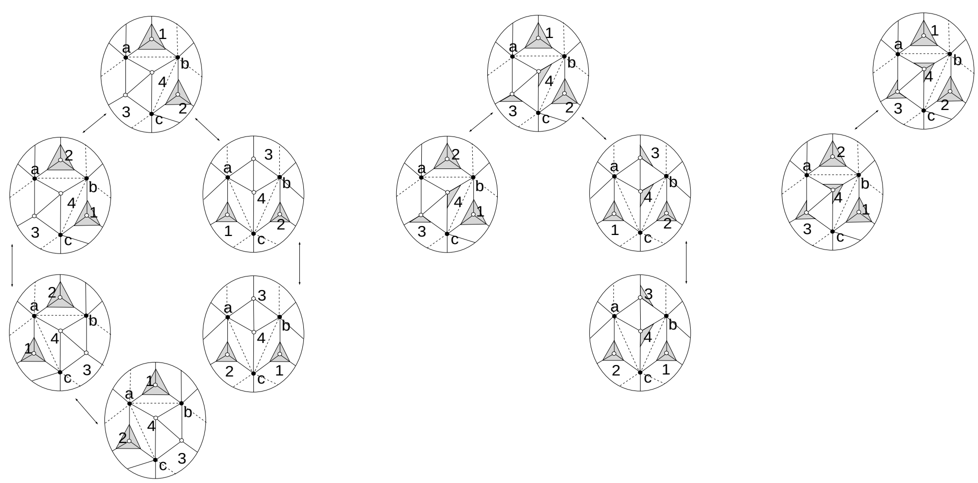

Figure 33.

Case 1.2.4.

Say that $B_3 \cup B_4 \neq \emptyset$. Any bridge in $B_3 \cup B_4$ can only exist in four of the six embeddings of H. So, without loss of generality, the bridges in $B_3 \cup B_4$ can be as shown on the top center or top right of Figure 33 depending on whether two or four of the possible embeddings of H extend to embeddings of all of G. These embeddings are related by the same Q-Twists as described earlier in this case.

Case 1.3 As in Case 1.2, we can assume without loss of generality that $\sigma_1|_H$ is the embedding of $K_{3,4}$ shown on the top of Figure 29. So now an H-bridge in $B_{(3,4)}$ is of one of the same four varieties: a single $(3,4)$-edge, an *a-corner*, a *c-corner*, or a quad bridge. Similarly, an H-bridge of $B_{(1,2)}$ is either a single $(1,2)$-edge, an *a-corner*, a *c-corner*, or a quad bridge.

If either $B_{(1,2)}$ or $B_{(3,4)}$ contains a quad bridge, then (without loss of generality) the same two embeddings for H are possible from Case 1.2.1. Again, the two embeddings of G will be related by flipping of edges in S and/or a Q-Twist hinged at a, c and latched at b. So we may assume that neither $B_{(1,2)}$ nor $B_{(3,4)}$ contains a quad bridge. In Case 1.3.1 assume that $B_{(1,2)} \cup B_{(3,4)}$ contains both a- and c-corners. In Case 1.3.2 $B_{(1,2)} \cup B_{(3,4)}$ contains only a-corners and no c-corners. In Case 1.3.3, $B_{(1,2)} \cup B_{(3,4)}$ contains neither a- nor c-corners.

Case 1.3.1 In this case, each of $B_{(1,2)}$ and $B_{(3,4)}$ may have both a- and c-corners or one has an a-corner but no c-corner and the other a c-corner but no a-corner. The possible embeddings of G with all possible bridges are shown in Figure 34 up to flipping of edges in S. The two embeddings are related by a Q-Twist hinged at a, c and latched at b with any placement of the edges in S.

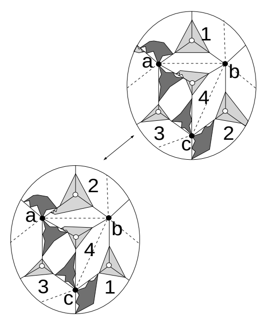

Figure 34.

Case 1.3.1.

Case 1.3.2 In this case, each of $B_{(1,2)}$ and $B_{(3,4)}$ may contain only a-corners. The four embeddings for H that allow for these a-corners are shown on the left in Figure 35. If all four embeddings for H extend to all of G, then these embeddings for G are shown on the left in Figure 35. The H-bridges in $B_3 \cup B_4$ further restrict the possible embeddings of H when they overlap with the a-corners such as what is shown on the right in Figure 35. (By symmetry the H-bridges of $B_1 \cup B_2$ may also restrict H to two reembeddings; furthermore if bridges in both $B_1 \cup B_2$ and $B_3 \cup B_4$ overlap, then there will be no reembeddings of H possible.) So without loss of generality all embeddings of G are shown in Figure 35 up to flipping of the (b, c)-edge. (There may also a $(1,2)$- or $(3,4)$-edges, and these may be treated as a-corners.)

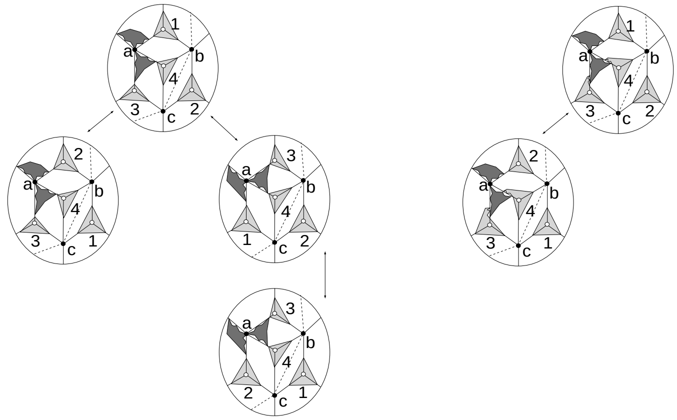

Figure 35.

Case 1.3.2.

The right-hand group of embeddings are related by flipping single edges and a Q-Twist hinged at a, c and latched at b. Consider the left-hand grouping of embeddings. The top embedding and the one to its left are related by a Q-Twist hinged at a, c and latched at b. The two embeddings on the right are related by a Q-Twist hinged at a, b and latched at c. The top embedding and the one to its right are related by a Q-Twist hinged at b, c, a_1, a_3 and latched at a_2, a_4 (where a_i is a vertex separating the a-corner from the B_i bridges).

Case 1.3.3 In this case $B_{(1,2)} \cup B_{(3,4)}$ consists of just the $(1, 2)$- and $(3, 4)$-edges. If $B_1 \cup B_2 \cup B_3 \cup B_4 \cup S = \emptyset$, then the embeddings of G are shown in Figure 36. The arrows in Figure 36 represent Q-Twists. The arrows between pairs of embeddings in which the $(3, 4)$-edges are parallel are related by a Q-Twist hinged at two vertices from $\{a, b, c\}$ and latched at the third. The vertical arrow on the left represents a full Q-Twist hinged at $a, 3, b, 1$ and latched at $2, 4$. The two remaining arrows similarly represent Q-Twists.

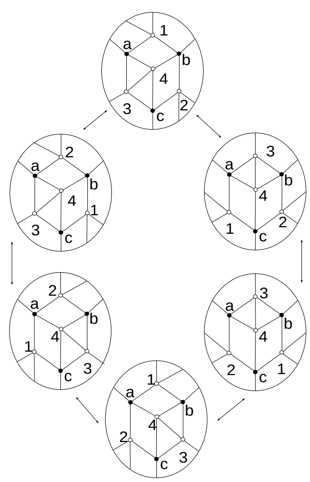

Figure 36.

Case 1.3.3.

If $B_1 \cup B_2 \cup B_3 \cup B_4 \cup S \neq \emptyset$, then out of the 6 possible embeddings of $H \cup (1, 2) \cup (3, 4)$ only 2 or 4 extend to all of G. In this case, we may consider the $(1, 2)$- and $(3, 4)$-edges as either a- or c-corners and finish as in Cases 1.3.1 and 1.3.2.

Case 2 Figure 37 shows the four embeddings of S_1 in the projective plane as extensions of the six embeddings of $K_{3,4}$ that we have been working with (two of the six embeddings of $K_{3,4}$ do not extend to embeddings of S_1).

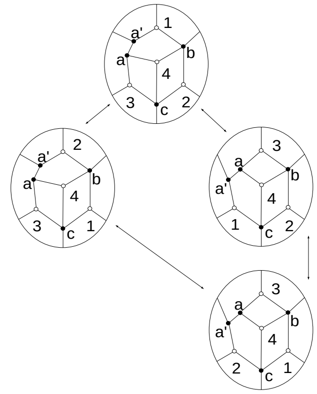

Figure 37.

The four embeddings of S_1 as extensions of the six embeddings of $K_{3,4}$.

Again we assume that $\sigma_1|_H$ is given by the top embedding shown in Figure 37. In Case 2.1 assume that $\sigma_2|_H = \sigma_1|_H$ and in Case 2.2 assume that $\sigma_2|_H \neq \sigma_1|_H$.

Case 2.1 Since $\sigma_2|_H = \sigma_1|_H$ (which is the top embedding in Figure 37), any difference between σ_1 and σ_2 would be a reembedded H-bridge that is a single (b, c)-edge or an H-bridge whose attachments are on b and the (a, a')-branch. That is, these latter reembeddable bridges form one or two "fans" with apex vertex b. Thus σ_1 and σ_2 are related by Q-Twists as in Case 1.1.3.1 of Section 4.

Case 2.2 We need only show how to go from an embedding of G with H as in the top of Figure 37 to an embedding of G with H as given by one of the other three. For each of the three cases, Figure 38 shows all of the possible H-bridges (aside from a single (b, c)-edge) that can occur in both embeddings of S_1.

For the left pair of embeddings, all possible H-bridges that can exist of both embeddings of S_1 are shown in the grey areas. The H-bridges in the two lighter grey areas have only one possible placement for each embedding of S_1, but a bridge in the darker grey fans have two possible placements for each embedding of S_1. We can go from any such embedding of the first type to some embedding of the second type by a degenerate Q-Twist hinged at x, c and latched at b. We then finish as in Case 2.1.

For the middle pair of embeddings, all possible H-bridges that can exist in both embeddings are within the grey areas shown aside from a single (b, c)-edge. Each such bridge (aside from the (b, c)-edge) has only one possible placement for each embedding of S_1. We go from the first to the second embedding shown by a Q-twist hinged at $1', 3', b, c$ and latched at $2', 4'$.

For the right pair of embeddings, all possible H-bridges are again in the grey areas. Each such bridge (aside from the (b, c)-edge) has only one possible placement for each embedding of S_1. We go from the first embedding to the second embedding by a degenerate P-Twist obtained from the central view of the P-Twist (see Figure 3) with vertex 4 in the center patch 7, the patches 0 and 9 contracted to make vertex c, and patches 3 and 4 contracted to make vertex b.

Figure 38.

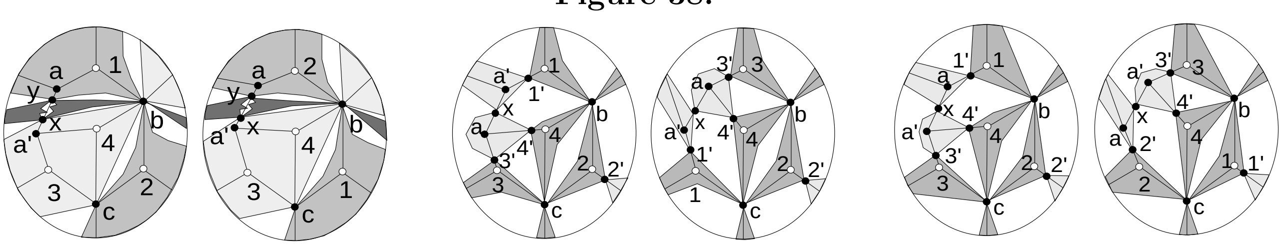

Case 2.2.

Case 3 In this case H is a subdivision of S_2. There are only two possible embeddings of S_2 in the projective plane and these are shown in Figure 39 ignoring the shaded grey regions. Either $\sigma_1|_H = \sigma_2|_H$

or $\sigma_1|_H \neq \sigma_2|_H$. In the former case, the difference between the two embeddings of G are the H-bridges in the four dark grey fans shown. The H-bridges in the lighter grey areas have only one possible placement with respect to the embedding for H. We can go between any two such embeddings by a sequence of Q-Twists as described in Case 1.1.3.1 of Section 4. In the latter case, we can go from σ_1 to σ_2 by a single Q-Twist hinged at a', b' and latched at c along with reembedding the fans as in Case 1.1.3.1 of Section 4.

Figure 39.

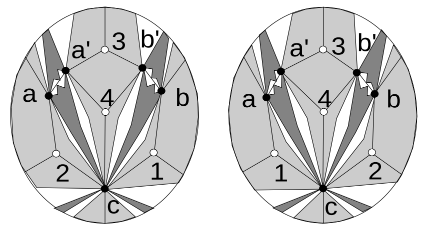

Case 3.

□

5.2 A 3-sum of two planar graphs

Let G be a 3-connected, non-planar graph that is embedded in the projective plane and G not internally 4-connected. Then there is a 3-sum $G = G_1 \oplus_3 G_2$. In this section we will prove Lemma 1.2 for the case for which G_1 and G_2 are both planar. Recall that a cycle in a graph is *peripheral* if it is chordless and non-separating. Also recall that in a 3-connected planar graph the peripheral cycles are exactly the facial cycles.

Proposition 5.2. *Suppose G is 3-connected, projective planar, nonplanar, and $G = G_1 \oplus_3 G_2$ where both G_1 and G_2 are planar. Then the triangle of summation is non-peripheral in at least one of G_1 and G_2. Furthermore, $G = K_3 \oplus_3 H_1 \oplus_3 H_2 \oplus_3 \cdots \oplus_3 H_k$ where $3 \leq k \leq 4$, each H_i is planar and summed into K_3, and the triangle of summation is peripheral in H_i.*

Proof. If the triangle of summation in $G_1 \oplus_3 G_2$ is peripheral in both, then $G = G_1 \oplus_3 G_2$ is planar, a contradiction. Supposing the triangle is not peripheral in G_1, we get that $G = K_3 \oplus_3 G_{1,1} \oplus_3 G_{1,2} \oplus_3 G_2$ where the sums are all at K_3. Repeating this process we get that $G = K_3 \oplus_3 H_1 \oplus_3 H_2 \oplus_3 \cdots \oplus_3 H_k$ in which each H_i is planar with its triangle of summation being peripheral and $k \geq 3$. We cannot have that $k \geq 5$ because then G will contain a $K_{3,5}$-minor, which is not projective planar, a contradiction. □

The embeddings of G for $k \in \{3, 4\}$ are depicted in Figure 40. If $k = 4$ in Proposition 5.2, then the 3-sum $G = G_1 \oplus_3 G_2$ splits a $K_{3,4}$ and so σ_1 and σ_2 are related by a sequence of Q-Twists and P-Twists by Proposition 5.1. If $k = 3$, then the fact that σ_1 and σ_2 are related by a sequence of Q-Twists follows by details similar to those (but much easier) presented in the proof of Proposition 5.1.

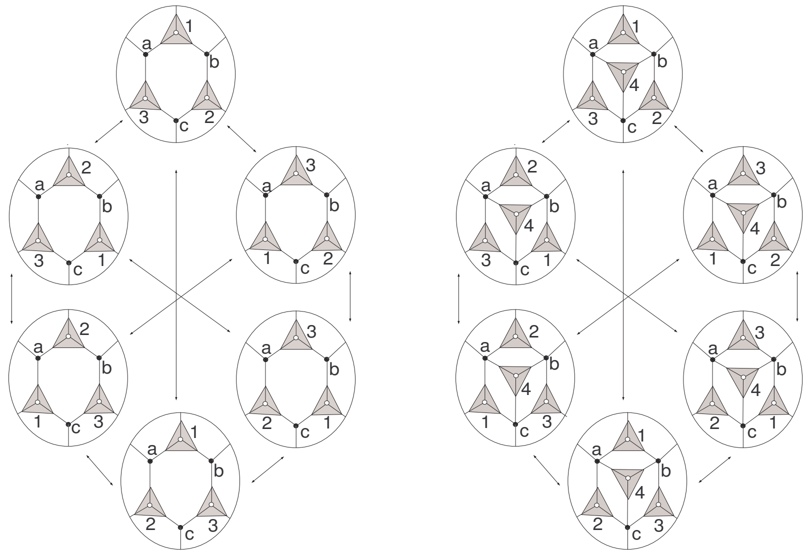

Figure 40.
Embeddings of 3-sums of planar graphs

5.3 A 3-sum of two non-planar graphs

In this section we prove Lemma 1.2 for the case that G is a 3-sum of two nonplanar graphs. The proof follows from Proposition 5.3. (We actually do not use the assumption that G is V_8-free in this section.)

Proposition 5.3. *If G is 3-connected and $G = G_1 \oplus_3 G_2$ where each G_i is nonplanar, then the 3-sum $G = G_1 \oplus_3 G_2$ splits a $K_{3,4}$ and we can go from any one embedding of G in the projective plane to any other embedding by a sequence of Q-Twists and P-Twists.*

Proof. Since each G_i is nonplanar and 3-connected, either $G_i \cong K_5$ or G_i contains a $K_{3,3}$-subdivision. From [18, 10.3.9], if G_i contains a $K_{3,3}$-subdivision, then G_i contains a minor from Figure 41 where the triangle of summation of G_i is shown in bold. In each case we have that 3-sum $G = G_1 \oplus_3 G_2$ splits a $K_{3,4}$ and so the rest of the result follows by Proposition 5.1.

Figure 41.

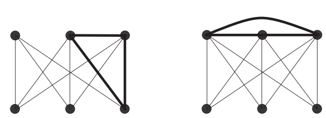

Triangles of summation in G_i

□

5.4 Reduction to an internally 4-connected frame

In this section we prove Lemma 1.2 for the case that G is V_8-free and cannot be written as a 3-sum of two planar graphs or as a 3-sum that splits a $K_{3,4}$. A 3-connected nonplanar graph G admits a *patch decomposition* with an internally 4-connected *frame* F_G and *patches* P_i when either G is internally 4-connected (and is its own frame with no patches) or $G = F_G \oplus_3 P_1 \oplus_3 P_2 \oplus_3 \cdots \oplus_3 P_k$ where

- F_G is an internally 4-connected, non-planar, and projective-planar graph,
- each 3-sum is not a ΔY-operation,
- each P_i is planar and summed onto a triangle of F_G,

- the triangle of summation is peripheral in P_i,
- no two P_i's are summed into the same triangle of F_G.

Proposition 5.4. *If G is 3-connected, nonplanar, and projective planar, then either G admits a patch decomposition, G is a 3-sum of two planar graphs, or $G = G_1 \oplus_3 G_2$ where the 3-sum splits a $K_{3,4}$.*

Proof. We proceed by induction on $|V(G)|+|E(G)|$. In the base case $|V(G)|+|E(G)| = 15$ and $G = K_5$ or $K_{3,3}$ and our result is immediate. So now say that $|V(G)| + |E(G)| > 15$ and assume that G is not a 3-sum of two planar graphs and $G \neq G_1 \oplus_3 G_2$ where the 3-sum splits a $K_{3,4}$. We will show that G admits a patch decomposition. If G is internally 4-connected, then we have our result. If not, then write $G = G' \oplus_3 P$ where the summation is along triangle T and the 3-sum is not a ΔY-operation. By assumption we cannot have that both G' and P are planar; furthermore, we cannot have that G' and P are both nonplanar because then the 3-sum would split a $K_{3,4}$ by Proposition 5.3. So assume that G' is nonplanar and P is planar. Rechoose G' and P so that the number of vertices in P is maximal. If T is not peripheral in P, then because P is planar we get that $P = P_1 \oplus_3 P_2$ where the 3-sum is on T and T is peripheral in each P_i; however, one can show (using the same techniques as in the proof of Proposition 5.3) that the 3-sum $G = G' \oplus_3 P$ splits a $K_{3,4}$. Hence T is peripheral in P.

By induction G' either admits a patch decomposition, is a 3-sum of two planar graphs, or can be expressed as a 3-sum that splits a $K_{3,4}$. The latter possibility, however, would imply that G is expressible as a 3-sum that splits a $K_{3,4}$, a contradiction of our assumptions about G. In Case 1 say that G' admits a patch decomposition and in Case 2 say that G' is a 3-sum of two planar graphs.

Case 1 Write the patch decomposition of G' as $G' = F_{G'} \oplus_3 Q_1 \oplus_3 Q_2 \oplus_3 \cdots \oplus_3 Q_m$. Let T_i be the triangle in $F_{G'}$ along which the summation with Q_i is taken. By the maximality of P, T is a triangle of $F_{G'}$ that is not on the same vertices of any T_i. Thus $G = F_{G'} \oplus_3 Q_1 \oplus_3 Q_2 \oplus_3 \cdots \oplus_3 Q_m \oplus_3 P$ which is a patch decomposition of G.

Case 2 We assume that $G' = G_1 \oplus_3 G_2$ where G_1 and G_2 are both planar. (Assume that $T \subset G_2$.) Rechoose G_1 and G_2 so that there is a maximum number of vertices in G_1 and $T \subset G_2$. Let T' be the triangle of summation for $G_1 \oplus_3 G_2$. Note that since G is not a 3-sum of two planar terms, it must be that $G_2 \oplus_3 P$ is nonplanar. Hence T is nonperipheral in G_2 because it is peripheral in P. Thus $G_2 = G_2' \oplus_3 G_2''$ summed along T where T' is in G_2'. See Figure 42. Of course $V(T)$ and $V(T')$ need not be disjoint.

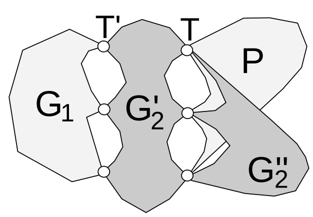

Figure 42.
Case 2: G' is a 3-sum of two planar graphs

Thus $G = (G_1 \oplus_3 G_2') \oplus_3 (G_2'' \oplus_3 P)$. It cannot be that $(G_2'' \oplus_3 P)$ is planar because of the maximality of P. This implies that T is not peripheral in G_2'' and so $G_2'' = H_1 \oplus_3 H_2$ where the 3-sum is again along T. Thus G can be expressed as a 3-sum (along $V(T)$) that splits a $K_{3,4}$, a contradiction. $\square$

Now consider a 3-connected, nonplanar, projective-planar graph G that has a patch decomposition $F_G \oplus_3 P_1 \oplus_3 P_2 \oplus_3 \cdots \oplus_3 P_k$. An embedding of F_G along with shaded triangular regions corresponding to $P_1 \setminus E(T_1), \ldots, P_k \setminus E(T_k)$ in the projective plane is called a *patch embedding* of $F_G \oplus_3 P_1 \oplus_3 P_2 \oplus_3 \cdots \oplus_3 P_k$.

Now note that F_G is a minor of G by 3-connectivity and the definition of 3-summing. Therefore, an embedding of G in the projective plane yields a unique induced embedding of F_G. Given this induced embedding of F_G, each $P_i \backslash E(T_i)$ can be replaced by a shaded triangular patch to yield a patch embedding of $F_G \oplus_3 P_1 \oplus_3 P_2 \oplus_3 \cdots \oplus_3 P_k$. Conversely a *patch embedding* of $F_G \oplus_3 P_1 \oplus_3 P_2 \oplus_3 \cdots \oplus_3 P_k$ yields a unique embedding of G in the projective plane (aside possibly from the edges of $E(T_i)$'s) by the fact that 3-connected planar graphs are uniquely embeddable in the plane. We do not get that patch embeddings of $F_G \oplus_3 P_1 \oplus_3 P_2 \oplus_3 \cdots \oplus_3 P_k$ uniquely correspond to embeddings of G; however, the only difference between the two are the placements of edges in the peripheral triangles of the P_i's. If such an edge $e \in E(T_i)$ that is also an edge of G does have more than one possible placement relative to a fixed embedding of F_G, then e lies along a 2-representative cut of the embedding of F_G that intersects F_G and G at the endpoints of e. Hence there are exactly two placements of e relative to a fixed embedding of F_G and $G \backslash e$ and these two placements are obtainable by flipping e (i.e., a degenerate Q-Twist). Thus Theorem 5.5 suffices to complete the proof of Lemma 1.2 for the case where G is V_8-free.

Theorem 5.5. *Let σ_1 and σ_2 be two patch embeddings of $F_G \oplus_3 P_1 \oplus_3 P_2 \oplus_3 \cdots \oplus_3 P_k$ in the projective plane, then we can go from σ_1 to σ_2 by a sequence of Q-Twists and P-Twists.*

The proof of Theorem 5.5 begins as follows. Since G does not contain a V_8-minor, neither does F_G (because F_G is a minor of G) and so Theorem 1.3 yields cases for the exact structure of F_G. In Section 5.4.1, we assume that F_G has five vertices; in Section 5.4.2, F_G is a double wheel; in Section 5.4.3, F_G has six vertices; in Section 5.4.4, F_G has seven vertices; in Section 5.4.8, F_G is 4-vertex coverable; and in Section 5.4.9, $F_G \cong L(K_{3,3})$.

5.4.1 Frames on five vertices

Given that F_G has five vertices and is nonplanar, we get that $F_G \cong K_5$. There are 27 distinct labeled embeddings of K_5 on the projective plane. Twelve of the 27 have a facial 5-cycle and the remaining 15 do not (see Figure 43).

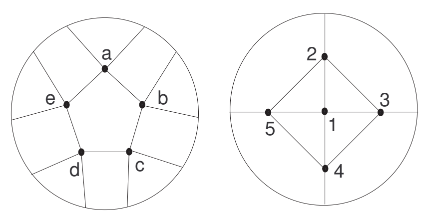

Figure 43.
Two classes of embeddings of K_5

Denote the embedding with facial 5-cycle a, b, c, d, e by $\sigma_{(abcde)}$. We need not consider the 15 embeddings without a facial 5-cycle by the following argument. If σ_1 induces an embedding of F_G as in the right of Figure 43, then because edges $(2,3)$ and $(4,5)$ form the diagonals of quadrilateral face $(3,5,2,4)$, either one of $(2,3)$ or $(4,5)$ can be flipped across the boundary by a degenerate Q-Twist because there can be at most two triangular patches in the face $(3,5,2,4)$. Thus we obtain a new patch embedding σ_1' with K_5 having a facial 5-cycle. So for the remainder of this section, we assume that both σ_1 and σ_2 are facial 5-cycle type embeddings.

Of the 12 embeddings of K_5 with a facial 5-cycle, the patches fall into two types: *outside patches* have their attachments on one of the 5 triangular faces of K_5 and *inside patches* do not. Outside patches may be embedded in either the interior or exterior of the pentagon, while inside patches must be embedded in the interior. When an outside patch is embedded inside the pentagonal face, it may be moved outside the pentagonal face by a degenerate Q-Twist. So we can assume that all outside patches are actually embedded outside the pentagonal face. This also has an advantage in that σ_1 and σ_2 are completely determined by their restrictions to K_5.

So without loss of generality we can assume that $\sigma_1 = \sigma_{(12345)}$. This is shown in the center of Figure 44. We can obtain the other 11 pentagonal embeddings of K_5 from $\sigma_{(12345)}$ by performing any permutation on 1,2,3,4,5 and then rotating so that vertex 1 is at the top and then possibly reflecting around a vertical axis through vertex 1. There are 10 2-cycle permutations in S_5 and these give rise to five distinct embeddings which are shown at a distance 1 from the center of Figure 44. There are 10 3-cycle permutations in S_5 and these give rise to another five distinct embeddings which are shown at a distance two from the center of Figure 44. The remaining two permutations in S_5 give the one remaining embedding, $\sigma_{(14253)}$. Since we have now accounted for all 12 pentagonal embeddings and have shown symmetry by 2-cycle and 3-cycle permutations, we can split the remainder of the proof in this section into three subcases: in Case 2.1, the permutations of σ_1 and σ_2 differ by a 2-cycle permutation; in Case 2.2, the permutations of σ_1 and σ_2 differ by a 3-cycle permutation; and in Case 2.3, $\sigma_2 = \sigma_{(14253)}$.

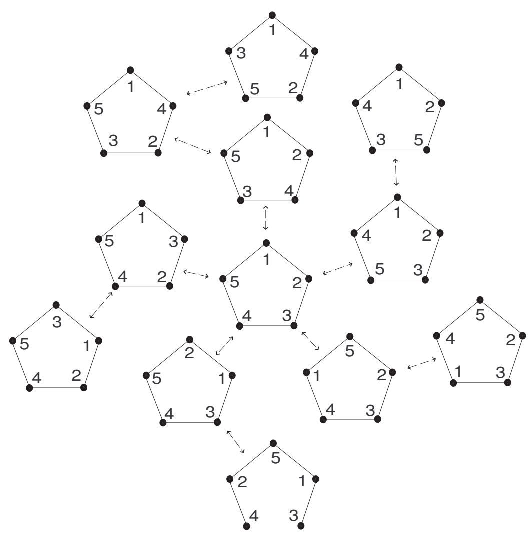

Figure 44.
Twelve embeddings of K_5 with a facial 5-cycle

In each case, we will find all of the maximal sets of patches that embed in both frame embeddings and then show how the two embeddings are related by a sequence of (degenerate) Q-Twists or P-Twists. Note that given two patches that could be both be placed in a particular embedding of K_5, they can embed simultaneously unless they are both inside patches and they both share two vertices of attachments that are consecutive along the 5-cycle.

Relative to the two frame embeddings, there are: *In-In patches* that are inside patches in both embeddings of K_5, *In-Out patches* that are inside patches in σ_1 and outside patches in σ_2, *Out-In Patches*, and *Out-Out Patches*.

Case 2.1 By renumbering and reflecting around a vertical axis, we can assume that $\sigma_2 = \sigma_{(12354)}$. Since outside patches have been moved to the exterior to the pentagon, we can assume that all Out-Out patches (i.e. $(1,3,4), (1,3,5)$ and $(2,4,5)$) exist.

There are three possible In-In patches, $(1,2,3)$, $(3,4,5)$, and $(1,4,5)$. In Case 2.1.1, say that the $(1,2,3)$-patch exists and in Case 2.1.2 say that it does not.

Case 2.1.1 Neither of the In-Out patches $(2,3,4)$ nor $(1,4,5)$ can exist in both σ_1 and σ_2 as they are blocked by the $(1,2,3)$-patch. Similarly, the Out-In Patches $(2,3,5)$ and $(1,2,4)$ cannot exist. Finally either of the remaining In-In patches $(3,4,5)$ and $(1,4,5)$ can exist, but not both simultaneously. Hence there are only two maximal patch structures in this case (and they are symmetric). See Figure 45. Note that a Q-Twist hinged at $1,5,4,3$ and latched at $2,3$ will take one embedding to the other.

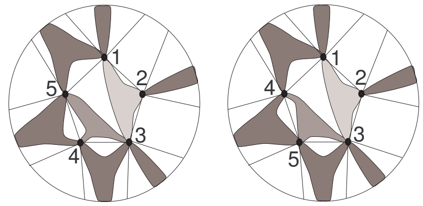

Figure 45.
$\sigma_{(12345)}$ and $\sigma_{(12354)}$ with In-In patches $(1,2,3)$ and $(3,4,5)$ - Related by a Q-Twist

Case 2.1.2 Here either the $(3,4,5)$-patch or $(1,4,5)$-patch may exist, but not both simultaneously. By symmetry we either have that the $(3,4,5)$-patch exists or there is no In-In patch.

In the first case, the only admissible patches are $(1,2,5)$ and $(1,2,4)$. Further they can both occur simultaneously. As can be seen in Figure 46, these embeddings are related by a Q-Twist hinged at $2,5,4,3$ and latched at $2,3$.

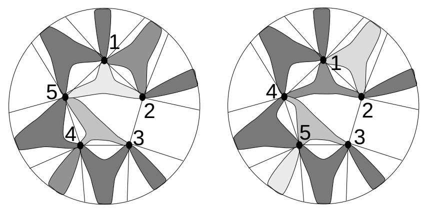

Figure 46.
$\sigma_{(12345)}$ and $\sigma_{(12354)}$ with patch $(3,4,5)$ - Related by a Q-Twist

In the second case, note that all four remaining patches can occur simultaneously as shown in Figure 47. The embeddings are related by a degenerate Q-Twist hinged at $4,5$ and latched at 2.

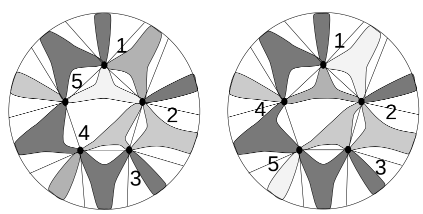

Figure 47.
$\sigma_{(12345)}$ and $\sigma_{(12354)}$ with no In-In Patch - Related by a Q-Twist

Case 2.2 By renumbering and reflecting around the vertical axis, we can assume that $\sigma_2 = \sigma_{(12453)}$. As before, we can assume that both Out-Out patches (i.e., $(1,3,4)$ and $(2,3,5)$) exist and are embedded on the outside of the 5-cycle. There are two possible In-In patches for σ_1 and σ_2: the $(1,2,3)$-patch and the $(3,4,5)$-patch: in Case 2.2.1, both of these patches exists; in Case 2.2.2, the $(1,2,3)$-patch exists and the $(3,4,5)$-patch does not; in Case 2.2.3, the $(1,2,3)$-patch does not exist and the $(3,4,5)$-patch does; and in Case 2.2.4, neither patch exists.
Case 2.2.1 Here none of the In-Out or Out-In patches can exist. This leads to the embeddings in Figure 48 which are related by a degenerate P-Twist. Consider the P-Twist in the Bowtie view from Figure 3. We obtain our desired degenerate P-Twist taking one embedding to the other as follows: Contract the patch labeled 1 to obtain node 1, contract the patch labeled 3 to obtain node 2, contract the two patches labeled 0 and 9 to obtain node 3, finally contract the edges on the patches labeled 2 and 4 that avoid the patches labeled 1 and 3 to obtain nodes 5 and 4 respectively.

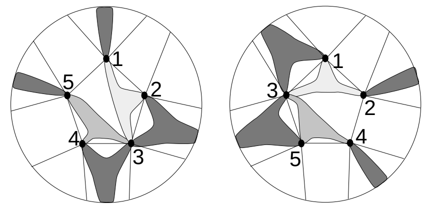

Figure 48.

$\sigma_{(12345)}$ and $\sigma_{(12453)}$ with both In-In Patches - Related By a P-Twist

Case 2.2.2 Here the only possible In-Out patch is $(1, 4, 5)$ and the only possible Out-In patch is $(2, 4, 5)$. Both can occur simultaneously. These two embeddings are shown in Figure 49. They are related by Q-Twists as follows. On the left embedding flip the $(1, 3, 4)$-patch, $(1, 3)$-edge, and $(1, 4)$-edge into the central pentagon. On the right embedding flip the $(2, 3, 5)$-patch, $(2, 3)$-edge, and $(2, 5)$-edge into the central pentagon. The resulting embeddings are the same because they both have the same central pentagon $(1, 2, 4, 3, 5)$ with no interior patches.

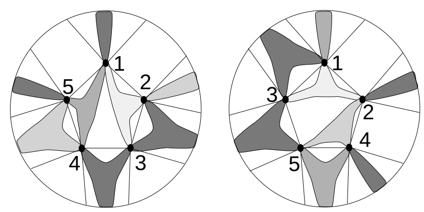

Figure 49.

$\sigma_{(12345)}$ and $\sigma_{(12453)}$ with five patches - Related by Q-Twists

Case 2.2.3 Here the only possible In-Out patch is $(1, 2, 5)$ and the only possible Out-In patch is $(1, 2, 4)$. Both can occur simultaneously. These two embeddings are related by a degenerate P-Twist as shown in Figure 50. Consider the P-Twist in the Bowtie view from Figure 3, then contract patches 1 and 2 to obtain vertex 2 and patch 9 to obtain vertex 5, contract the edge of patch 3 that avoids patch 8, the edge of patch 6 that avoids patch 2, and the edge of patch 0 that avoids patch 9.

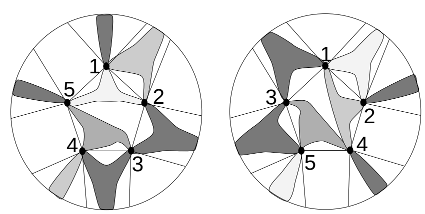

Figure 50.

$\sigma_{(12345)}$ and $\sigma_{(12453)}$ with five patches - Related by a P-Twist

Case 2.2.4 There are three In-Out patches and three Out-In patches to consider. It is clear that the maximal possible patch sets of In-Out patches are $\{(2, 3, 4), (4, 5, 1)\}$ and $\{(2, 3, 4), (1, 2, 5)\}$; similarly, the maximal possible patch sets of Out-In patches are $\{(1, 3, 5), (1, 2, 4)\}$ and $\{(1, 3, 5), (2, 4, 5)\}$. Furthermore, these maximal possibilities can occur simultaneously. This leads to four pairs of embeddings, each happen to be symmetric. One such pair is shown in Figure 51. They are related by a single Q-Twist hinged on 1,2,4,5 and latched on 1,4.

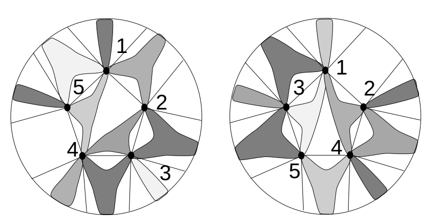

Figure 51.

$\sigma_{(12345)}$ and $\sigma_{(12453)}$ with no In-In Patches - Related by a Q-Twist

Case 2.3 By renumbering and reflecting around the vertical axis, we can assume that $\sigma_2 = \sigma_{(14253)}$.In this case, there are no Out-Out patches and no In-In patches possible. There are five possible In-Out patches $\{(1,2,3), (2,3,4), (3,4,5), (4,5,1), (5,1,2)\}$ and five possible Out-In patches $\{(1,4,2), (4,2,5), (2,5,3), (5,3,1), (3,1,4)\}$ for the pair of embeddings. Moreover, any patch from one set can embed simultaneously with any patch from the second.

So without loss of generality, we assume that $(1,2,3)$ exists in the patch structure. There are two possible In-Out patches that can also occur, $(3,4,5)$ and $(4,5,1)$. By symmetry, we can assume that $(3,4,5)$ occurs. Similarly, we consider the pairs of Out-In patches that occur. Up to symmetry and reversing σ_1 and σ_2, there are only two maximal structure that occurs: $(1,2,3),(3,4,5)$, $(2,3,5)$ and $(1,2,4)$ as shown in Figure 52, and $(1,2,3),(3,4,5)$, $(2,3,5)$ and $(1,3,4)$ as shown on the left in Figure 53. The first pair of patch embeddings are related by a P-Twist obtained from the Bowtie view in Figure 3, as follows: Contract patch 1 to obtain node 1, contract patch 3 to obtain node 2, contract patches 0 and 9 to obtain node 3, contact the edge of patch 4 that avoids patch 3 to obtain node 4, finally contract the edge of patch 2 that avoids patch 2 to obtain node 5. The patches $4, 5, 6$ and 7 remain. The leftmost patch embedding in Figure 53 is related to the rightmost embedding in the figure by flipping the $(1,3)$- and $(3,5)$-edges into the central pentagon. The reembedding from the middle embedding to the right embedding is the same reembedding as in Figure 48.

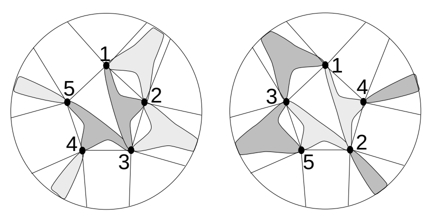

Figure 52.
$\sigma_{(12345)}$ and $\sigma_{(13524)}$ with patches $(1,2,3),(3,4,5)$, $(2,3,5)$ and $(1,2,4)$ - Related by a P-Twist

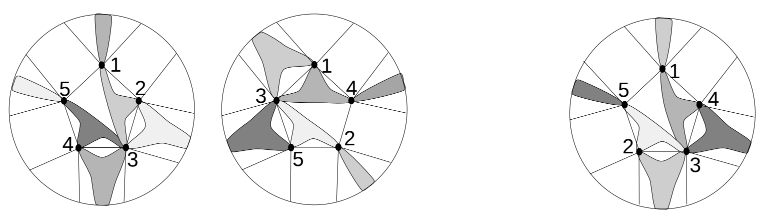

Figure 53.

$\sigma_{(12345)}$ and $\sigma_{(13524)}$ with patches $(1,2,3),(3,4,5)$, $(2,3,5)$ and $(1,3,4)$
Related by a Q-twist then a P-Twist

5.4.2 Frames that are subgraphs of double wheels

Let DW_n denote the double wheel graph with adjacent hub vertices whose rim has length n. Assume that F_G is isomorphic to an internally 4-connected subgraph of DW_n. Note that $DW_3 \cong K_5$, which was analyzed in Section 5.4.1. Hence we assume that $n \geq 4$. Assume that $v_1, v_2, \ldots, v_n$ are the vertices of the rim R in cyclic order and call the hub vertices a and b.

We assume that the projective plane is rendered as a disk with boundary covered by $\underline{v_1}, \ldots, \underline{v_n}, \overline{v_1}, \ldots, \overline{v_n}$ where $\underline{v_i} = \overline{v_i} = v_i$ but where the underlined vertices are along the top half of the disk and the overlined vertices are along the bottom half of the disk. In Figure 54 we show eight different embeddings of DW_n rendered in this way. Let ν_i be the embedding with two quadrangular faces on $\{v_i, v_{i-1}, a, b\}$. The embeddings ν_1 and ν_2 are shown in Figure 54. Let $\nu_{i,a}$ be the embedding obtained from ν_i by reembedding the av_i-spoke and define $\nu_{i,b}$ similarly: the embeddings $\nu_{n,a}$, $\nu_{n,b}$, $\nu_{1,a}$, $\nu_{1,b}$, $\nu_{2,a}$, and $\nu_{2,b}$ are also shown in Figure 54. If both av_i- and bv_i-spokes are reembedded, the resulting embedding is ν_{i+1}. One can show that there is no embedding of DW_n for $n \geq 4$ such that the rim cycle separates the projective plane and hence these $3n$ embeddings of DW_n are all the possible embeddings.

Deleting the ab-hub-edge or any rim edge from DW_n results in a planar graph. So for n even, the only internally 4-connected non-planar spanning subgraph G of DW_n is obtained by deleting spokes av_{2t-1} and bv_{2t} for all $1 \leq t \leq \frac{n}{2}$; call this subgraph AW_n. For n odd, one can show that there are no internally 4-connected non-planar subgraphs. Note that if $F_G \cong AW_4 \cong K_{3,3}$, then this case will be analyzed in Section 5.4.3. Hence for this section, we can assume that F_G is isomorphic to DW_n for $n \geq 4$ or AW_n for $n \geq 6$ and n even.

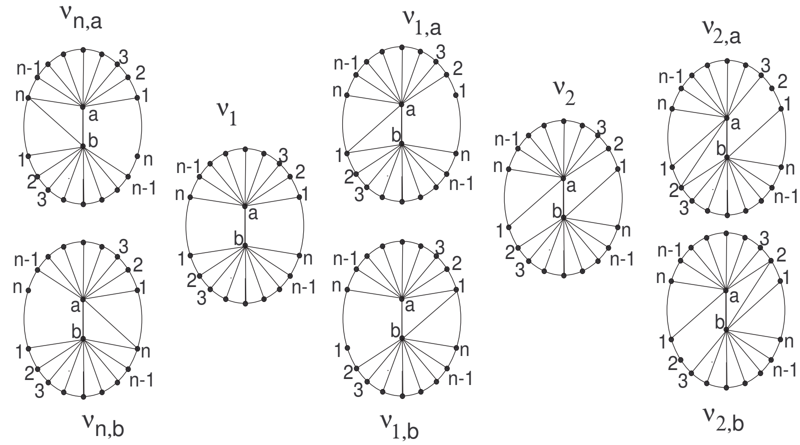

Figure 54.

Some Reembedings of Double Wheels

In this and subsequent sections, we will often show that a certain patch structure on a frame graph F_G will give rise to a subdivision of V_8 in the graph G. In these cases, we can refer back to the proof in Section 4 to complete the proof.

First, suppose σ_1 and σ_2 are two patch embeddings of $F_G = AW_m$ for $m \geq 6$. Note that for any embedding of AW_n with $n \geq 6$ the rim R must be non-contractible. Furthermore, $\nu_{i,a}$ restricted to AW_n is the same as ν_{i+1} restricted to AW_n. Thus the only embeddings of AW_n are $\nu_1, \ldots, \nu_n$ restricted to AW_n. Also since AW_n has no triangles, it has no patches. So if $\sigma_1 = \nu_j$ and $\sigma_2 = \nu_k$, we can take σ_1 to σ_2 by a sequence of degenerate Q-Twists that move one spoke of the wheel at a time.

Now suppose σ_1 and σ_2 are two patch embeddings of $F_G = DW_n$ for $n \geq 4$. There are two types of patches possible in these embeddings of DW_n, *hub patches* on (a, b, v_j) and *rim patches* on (a, v_j, v_{j+1}) or (b, v_j, v_{j+1}). In Case 1 say that $n \geq 5$ and in Case 2 say that $n = 4$.

Case 1 Label the rim vertices of DW_5 by 1,2,3,4,5 and the hub vertices by 6,7. If we perform a ΔY-operation on triangle $1, 6, 7$ and then delete edges $(2, 6), (4, 6), (3, 7), (5, 7)$ we obtain V_8. Thus any hub patch on $F_G \cong DW_n$ implies that G has a V_8-minor and so we assume there are no hub patches on F_G. Also if we double the $(1, 2)$-edge and then perform ΔY-operations on triangles 1,2,6 and 1,2,7, then we can contract the $(2, 3)$-edge and delete edges $(3, 6), (4, 6), (3, 7), (5, 7)$ to obtain V_8. Thus any two rim patches (a, v_j, v_{j+1}) and (b, v_j, v_{j+1}) on F_G will imply that G has a V_8-minor and so we assume that there are no two such patches. So now for each rim edge (v_{j-1}, v_j) either there is no rim patch on (v_{j-1}, v_j), a single (v_{j-1}, v_j, a)-patch, a single (v_{j-1}, v_j, b)-patch, but not both rim patches. Furthermore, note that a (v_{j-1}, v_j, a)-patch is has only one possible placement in any embedding of DW_n save for $\nu_{j-1,b}$, ν_j, and $\nu_{j,a}$. In a given embedding of DW_n, two rim patches with nonadjacent rim edges cannot both be reembedded. Similarly, two rim patches with adjacent rim edges and the same hub vertex cannot both be reembedded. Two rim patches with adjacent rim edges and different hub vertices are both flexible in a single embedding of DW_n. Figure 55 shows all of the possible patch embeddings for DW_n with a (v_n, v_1, a)-patch and (v_1, v_2, b)-patch in the five embeddings of DW_n in which one or both patches are reembeddable.

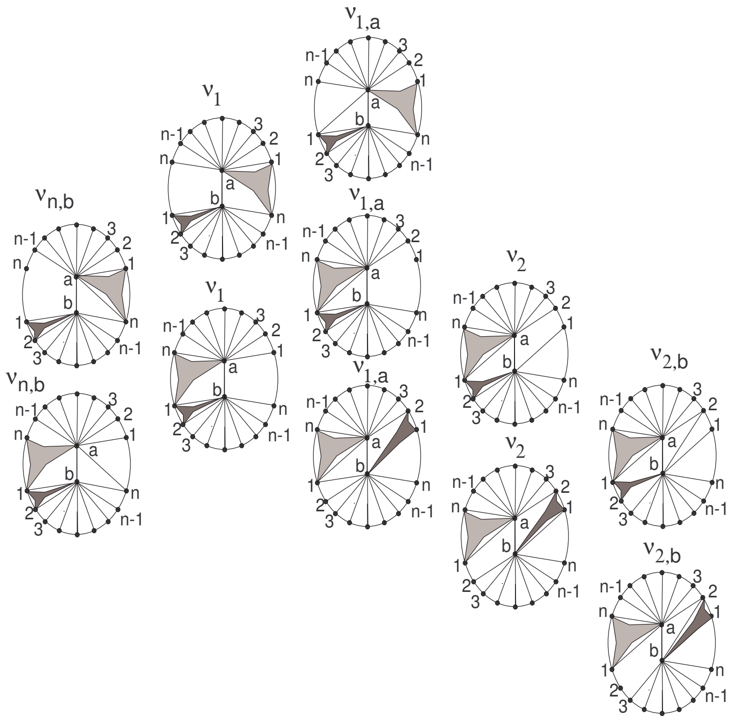

Figure 55.
Patch embeddings for DW_n with two adjacent rim patches

So we see that any patch embedding of DW_n without two patches on the same rim edge may use any embedding of the frame DW_n. When any single patch or any single edge of DW_n is reembeddable, they may be reembedded individually by Q-Twists in a certain order. When multiple rim patches and single edges are reembeddable, the possible embeddings are shown in Figure 55 where again we see that we may always reembed patches and edges individually to get from one embedding to another.

Case 2 First we give some patch configurations on DW_4 that produce a V_8-minor in G. For this discussion label the rim vertices of DW_4 with 1,2,3,4 and hub vertices with a,b.

First, any hub patch and rim patch together create a V_8-minor. To see this perform ΔY-operations on triangles $(1, 2, a)$ and $(4, a, b)$ and delete the $(3, b)$-edge to obtain V_8. Next perform ΔY-operations on triangles $(1, 2, a)$ and $(1, a, b)$ and delete the $(4, a)$- and $(3, b)$-edges to obtain V_8.

Second, any two hub patches with adjacent rim vertices together create a V_8-minor. To see this perform ΔY-operations on the triangles $(1, a, b)$ and $(2, a, b)$ and delete the $(3, a)$- and $(4, b)$-edges to obtain V_8. Note also that it is not possible at all to embed two hub patches with nonadjacent rim vertices.

So now the only possible patch configurations that do not produce a V_8-minor in G are a single hub patch or solely rim patches. In the latter case, we obtain the result that any two patch embeddings are related by Q-Twists as in Case 1. In the former case, consider Figure 56 which shows all possible patch embeddings of DW_4 with the single hub patch $(1, a, b)$. One can see that these embeddings are all related by Q-Twists.

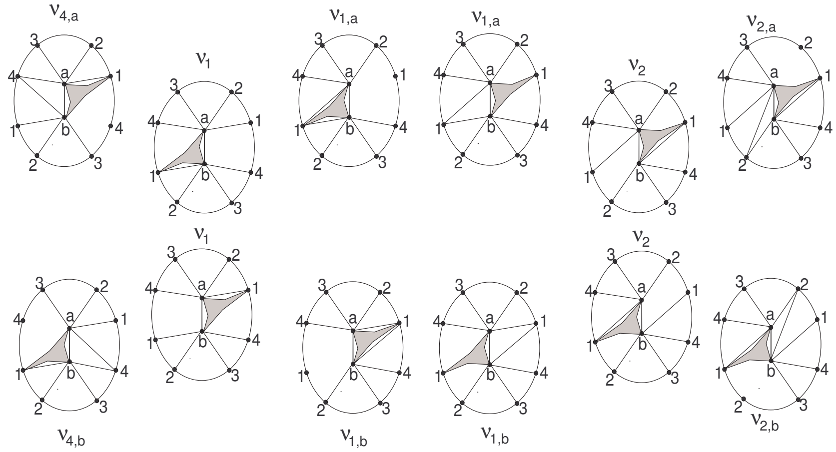

Figure 56.

Possible patch embeddings of DW_4

5.4.3 Frames on six vertices

In each of Sections 5.4.3–5.4.8, we will use the following naming conventions for the many graphs needed in the analysis. Given two graphs G and H, GH will denote the disjoint union while $\overline{G}$ will denote the complement of G. For k a positive integer, C_k will be the cycle on k edges, P_k will be the path on k edges, M_k will be the matching graph on k edges, K_k will be the complete graph on k vertices, and E_k will be the edgeless graph on k vertices. Let N_4 be the graph consisting of a triangle with a pendant edge. Let B_7, the bowtie graph, be obtained by identifying the vertices of degree one in two copies of N_4.

There are four internally 4-connected nonplanar graphs on six vertices: K_6, $K_6\backslash e$, DW_4, and $K_{3,3}$. We have analyzed the case where $F_G \cong DW_4$ in Section 5.4.2 on double wheels. In the case that $F_G \cong K_{3,3}$, there are no patches because $K_{3,3}$ has no triangles. There are six embeddings of $K_{3,3}$ and they are shown in Figure 40 and they are all related by Q-Twists. So we need only analyze the cases for K_6 and $K_6\backslash e$. Let these be Cases 1 and 2, respectively.

Case 1 There is a unique unlabeled projective-planar embedding of K_6, which is a triangulation. If there are no patches on the frame, then there are twelve distinct embeddings. To see this consider the vertex 0 fixed in the center of a 5-cycle. Vitray [19, Thm.5.2.3] showed that a Q-twist on such an embedding has the effect of transposing two vertices on the 5-cycle. Hence, any embedding of K_6 with no patches can be obtained from any other embedding by a sequence of Q-Twists. Note that a given patch might not be allowable in one of the intermediate embeddings in the sequence.

To analyze the possible patch structures, label the vertices $0, 1, 2, 3, 4, 5$. In Figure 57 we show the six possible labeled embeddings where $0, 1, 5$ is a facial triangle and $2, 3, 4$ is a noncontractible cycle. The remaining six embeddings of K_6 have $2, 3, 4$ as a facial triangle and $0, 1, 5$ as a noncontractible cycle.

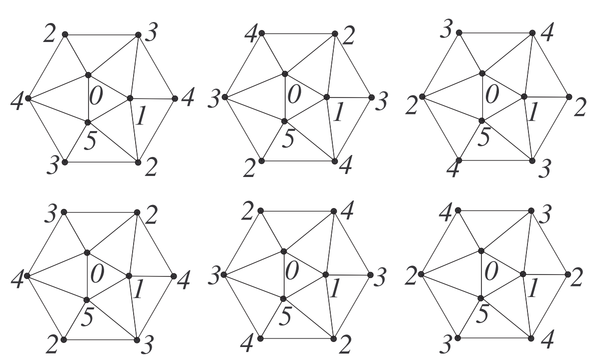

Figure 57.

Six possible embeddings of K_6

Without loss of generality assume there is a $(0,1,5)$-patch. So we can assume that each of σ_1 and σ_2 is one of the embeddings shown in Figure 57. Since K_6 is 3-representative in the projective plane, any patch has only one possible placement. This implies that any two patch embeddings of K_6 with the same underlying embedding of K_6 and the same set of patches are the same patch embeddings. So without loss of generality assume we have patch embedding σ_1 with K_6 as shown in the upper left of Figure 57. Up to symmetry there are two types of frame embeddings possible for σ_2, one with a transposition on the boundary and one with a rotation on the boundary. These two patch embeddings are shown with the maximal patch structures in Figure 58.

Figure 58.

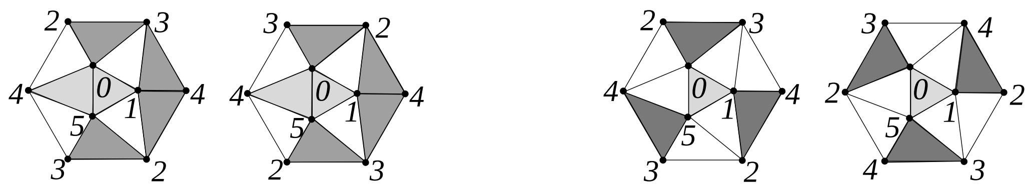

Two maximal patch structures on K_6

The reembedding on the left is a Q-Twist hinged at $0,2,3,5$ and latched at $1,4$ (and then reflected along a horizontal line). The reembedding on the right is a degenerate P-Twist obtained from the central view of the P-Twist (see Figure 3) by contracting patches 6 and 2 to an edge, patches 3 and 8 to an edge, and patches 5 and 9 to an edge.

Case 2 Suppose $F_G \cong K_6 \backslash e$, K_6 with the edge $(1,2)$ removed. There are two types of embeddings of this graph: those that extend to an embedding of K_6 and those that do not. There are twelve embeddings of the first type and six of the latter type which are shown in Figure 59. In each of these six embeddings the embedding of the K_4 induced on $\{3,4,5,6\}$ can be assumed to be fixed.

Figure 59.

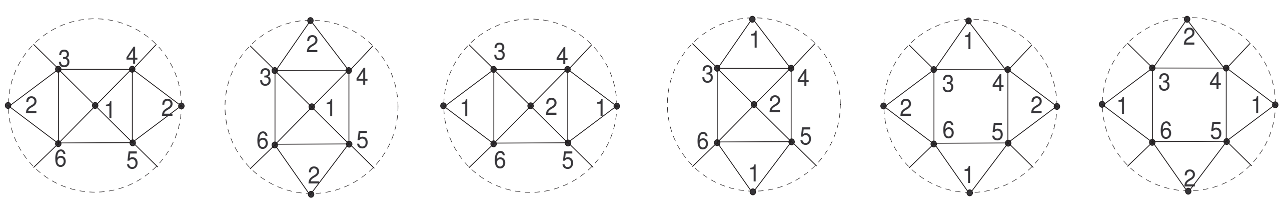

Six of the eighteen embeddings of $K_6 \backslash e$

Given any patch embedding of $F_G = K_6 \backslash e$, if the frame is embedded in an extendable fashion, then the quadrilateral face of F_G bounded by vertices $1,u,2,v$ cannot have a $(1,2,u)$- or $(1,2,v)$-patch because these are not triangles in F_G. Thus we can flip the (u,v)-edge into the quadrilateral and so F_G is now embedded in a nonextendable fashion. Therefore we can assume that we have patch embeddings σ_1 and σ_2 with the embeddings of F_G as in Figure 59. After relabeling, we can assume that $\sigma_1|_{F_G}$ is the leftmost embedding in Figure 59 and so $\sigma_2|_{F_G}$ is one of the first through sixth embeddings shown in the figure. Let these be Cases 2.1–2.6, respectively. In each case notice that there are exactly two 2-representative cuts in each of the embeddings of F_G and no cut can be moved off a vertex onto an incident edge. Thus the placement of patches is uniquely determined in each embedding of F_G.

Case 2.1 Here we must have $\sigma_1 = \sigma_2$ as any patch is embedded in a unique face of $\sigma_1|_{K_6 \backslash e}$.

Case 2.2 The patches that can exist along with F_G in both $\sigma_1|_{F_G}$ and $\sigma_2|_{F_G}$ are on $(1,3,4)$, $(1,4,5)$, $(1,5,6)$, $(1,3,6)$, $(2,4,6)$, and $(2,3,5)$. Furthermore, all of these patches may be embedded simultaneously and we assume that they are. Now one can move from σ_1 to σ_2 by a Q-Twist hinged at 3,4,5,6 and latched at 2.
Case 2.3 The patches that can exist along with F_G in both $\sigma_1|_{F_G}$ and $\sigma_2|_{F_G}$ are on $(1,4,5)$, $(2,4,5)$, $(1,3,6)$, and $(2,3,6)$. Furthermore, all of these patches may be embedded simultaneously and we assume that they are. Now one can move from σ_1 to σ_2 by a Q-Twist hinged at 3,4,5,6 and latched at 1,2.
Case 2.4 The patches that can exist along with F_G in both $\sigma_1|_{F_G}$ and $\sigma_2|_{F_G}$ are on $(1,3,4)$, $(1,5,6)$, $(2,4,5)$, and $(2,3,6)$. Furthermore, all of these patches may be embedded simultaneously and we assume that they are. Now one can move from σ_1 to σ_2 by two Q-Twists which are both hinged at 3,4,5,6; the first twist is latched at 1 and the second twist is latched at 2.
Case 2.5 The patches that can exist along with F_G in both $\sigma_1|_{F_G}$ and $\sigma_2|_{F_G}$ are on $(1,3,4)$, $(1,5,6)$, $(2,4,5)$, $(2,3,6)$, $(2,4,6)$, and $(2,3,5)$. Furthermore, all of these patches may be embedded simultaneously and we assume that they are. Now one can move from σ_1 to σ_2 by a Q-Twist hinged at 3,4,5,6 and latched at 1.
Case 2.6 The patches that can exist along with F_G in both $\sigma_1|_{F_G}$ and $\sigma_2|_{F_G}$ are on $(1,3,6)$, $(1,4,5)$, $(2,4,6)$, and $(2,3,5)$. Furthermore, all of these patches may be embedded simultaneously and we assume that they are. Now one can move from σ_1 to σ_2 by two Q-Twists which are both hinged at 3,4,5,6; the first twist is latched at 2 and the second twist is latched at 1.

5.4.4 Frames on seven vertices

In this section, we assume that F_G has seven vertices.

Proposition 5.6. *There are exactly 28 internally* 4*-connected graphs on seven vertices. Of these graphs, one is planar and seven are not projective planar.*

Proof. Let G be an internally-4-connected graph on seven vertices. If $\delta(G) = 6$, then G must be isomorphic to K_7. If $\delta(G) = 5$, then $\Delta(\overline{G}) = 1$. Hence G is isomorphic to either $\overline{M_1E_5}$, $\overline{M_2E_3}$ or $\overline{M_3E_1}$, which are all internally 4-connected. In the case when $\delta(G) = 4$, as $\overline{C_4E_3}, \overline{C_4M_1E_1}, \overline{C_4P_2}$ and $\overline{C_4C_3}$ are not internally-4-connected, G must be one of the following 21 graphs: $\overline{C_3E_4}$, $\overline{C_5E_2}$, $\overline{C_6E_1}$, $\overline{C_7}$, $\overline{P_2E_4}$, $\overline{P_3E_3}$, $\overline{P_4E_2}$, $\overline{P_5E_1}$, $\overline{P_6}$, $\overline{C_3C_3E_1}$, $\overline{P_2P_2E_1}$, $\overline{P_2P_3}$, $\overline{C_3P_2E_1}$, $\overline{C_3P_3}$, $\overline{C_3M_1E_2}$, $\overline{C_3M_2}$, $\overline{C_5M_1}$, $\overline{P_2M_1E_2}$, $\overline{P_2M_2}$, $\overline{P_3M_1E_1}$, and $\overline{P_4M_1}$.

Finally, in the case $\delta(G) = 3$, let v be a 3-valent vertex and label the neighbors of v as $1, 2, 3$ and the remaining three vertices as a, b, c. By internal 4-connectivity, vertices $1, 2, 3$ are independent. Vertex 1 must then be adjacent to at least two of a, b, c. If 1 is only adjacent to a and b, then by internal 4-connectivity a and b are nonadjacent. In order to excluded 3-separations with five vertices on each side we now must have that c is adjacent to both a and b; furthermore, 2 and 3 are both adjacent to all of a, b, c. Thus $G = \overline{B_7}$. If vertex 1 has degree 4, then without loss of generality vertices 2 and 3 both have degree 4 and since $K_{3,4}$ is not internally 4-connected we now get that $G = \overline{C_3K_{1,3}}$ or $G = \overline{C_3N_4}$.

Note that $\overline{C_5M_1}$ is a planar double wheel. Further, $\overline{M_3E_1}$ and $\overline{P_4E_2}$ are isomorphic to A_2 and B_1, respectively, in Archdeacon's list of 35 minor-minimal non-projective-planar graphs (see, e.g., [9]). Hence, $\overline{M_3E_1}$, $\overline{P_4E_2}$, $\overline{M_2E_3}$, $\overline{M_1E_5}$, $\overline{P_3E_3}$, $\overline{P_2E_4}$ and K_7 are all not projective-planar. □

Hence we need to consider the flexibility of graphs G whose frame F_G is isomorphic to one of the graphs in the set $\mathcal{L}$ which consists of the 20 internally 4-connected projective planar, non-planar graphs listed in the proof of Proposition 5.6. We will analyze these graphs according to whether they contain a $K_{3,4}$-subgraph, a $\overline{C_7}$-subgraph, or neither.

There are 13 graphs in $\mathcal{L}$ that contain a $K_{3,4}$-subgraph: $\overline{C_3E_4}$, $\overline{P_2M_1E_2}$, $\overline{C_3M_1E_2}$, $\overline{P_3M_1E_1}$, $\overline{P_2P_2E_1}$, $\overline{P_2M_2}$, $\overline{C_3P_2E_1}$, $\overline{C_3M_2}$, $\overline{P_2P_3}$, $\overline{C_3C_3E_1}$, $\overline{C_3P_3}$, $\overline{C_3K_{1,3}}$ and $\overline{C_3N_4}$. These 13 graphs will be analyzed in Section 5.4.5

There are four graphs in $\mathcal{L}$ that do not contain a $K_{3,4}$-subgraph but contain a $\overline{C_7}$: $\overline{C_7}, \overline{P_6}, \overline{P_5E_1}$, and $\overline{P_4M_1}$. These four graphs will be analyzed in Section 5.4.6.

There are three remaining graphs in $\mathcal{L}$: $\overline{C_6E_1}, \overline{C_5E_2}$ and $\overline{B_7}$. These three graphs will be analyzed in Section 5.4.7.

5.4.5 Frames that contain a $K_{3,4}$ subgraph

First, we consider the case when F_G is isomorphic to one of the 13 graphs in $\mathcal{L}$ that contain a $K_{3,4}$-subgraph. The six embeddings of $K_{3,4}$ are shown on the left of Figure 60 where the arrows represent relation by a single Q-Twist. Label the vertices of the two partite sets of the $K_{3,4}$-subgraph are $\{1, 2, 3\}$ and $\{4, 5, 6, 7\}$. In Case 1, we will consider the case when vertices $1, 2, 3$ are independent. In Case 2, we will consider the case when there is at least one edge in $\{1, 2, 3\}$.

Case 1 Here $K_{3,4} \subseteq F_G \subseteq \overline{C_3E_4}$. Consider one edge, call it e, of the six possible edges connecting two vertices from $\{4, 5, 6, 7\}$. In each of the six embeddings of $K_{3,4}$, there is only one possible placement for e. Furthermore all six of these edges may be embedded simultaneously in any of the six embeddings of $K_{3,4}$. These embeddings are shown on the right of Figure 60. The only 2-representative cuts of an embedding of $K_{3,4}$ pass through two of the vertices $\{1, 2, 3\}$. In particular, there are no 2-representative cuts that pass through the interior of an edge. As such any patch on F_G has a unique placement in any embedding of F_G. Therefore, we may assume that $F_G = \overline{C_3E_4}$ without losing any possible embeddings of patch graphs with $F_G \subset \overline{C_3E_4}$.

Any two embeddings of F_G are related by either a single Q-Twist or a single P-Twist. The arrows in Figure 60 represent Q-Twists similar to the one shown on the top right of the figure for $\overline{C_3E_4}$ latched at $\{4, 6\}$ and hinged at $\{2, 3, 5, 7\}$ which transpose the vertices in 2 and 3. Any patches on F_G common to both of these embeddings are preserved by this Q-Twist. For two embeddings not connected by an arrow (without loss of generality we may consider the top left embedding and the lower embedding) the possible patches that can exist along with both embeddings of F_G are shown in Figure 61. There is a degenerate P-Twist that takes one embedding to the other. This can be seen by contracting patches $0, 1, 4, 7$ in the central view of the P-Twist structure shown in Figure 3.

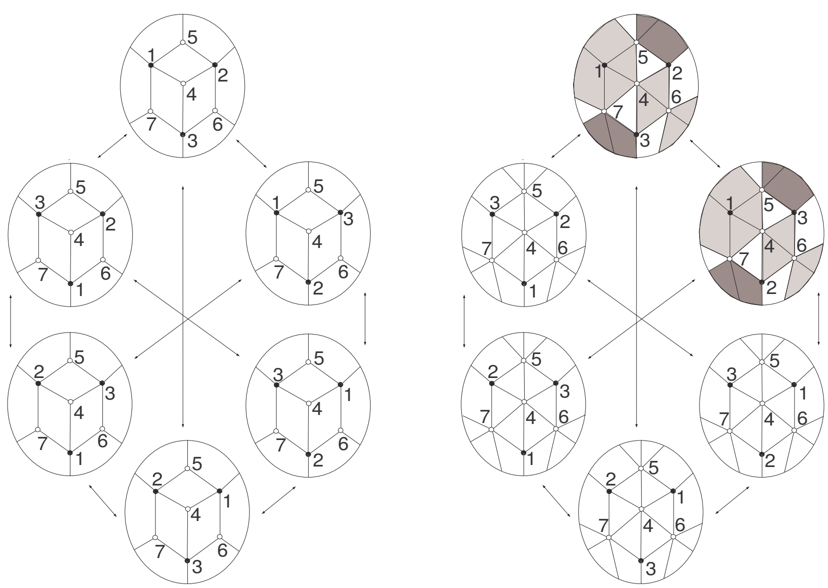

Figure 60.
Flexibility of $K_{3,4}$ and $\overline{C_3E_4}$ by Q-Twists

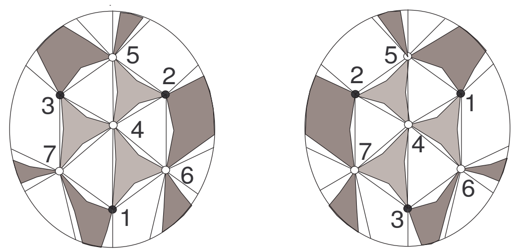

Figure 61.
Rotations of $\{1,2,3\}$ in $\overline{C_3E_4}$ by Degenerate P-Twist

Case 2 Of the 13 graphs contained in $\mathcal{L}$ that contain a $K_{3,4}$-subgraph, it remains to consider the case when F_G is isomorphic to one of those graphs that contain at least one edge on the vertices $\{1,2,3\}$. These are the five graphs: $\overline{P_2M_1E_2}$, $\overline{P_3M_1E_1}$, $\overline{P_2P_2E_1}$, $\overline{P_2P_3}$ and $\overline{P_2M_2}$. These will be Cases 2.1–2.5 respectively.
Case 2.1 Let $F_G = \overline{P_2M_1E_2}$ where P_2 is on vertices $\{1,2,3\}$ and M_1E_2 is on vertices $\{4,5,6,7\}$. We may assume without loss of generality that M_1 is the $(4,5)$-edge. As before, each of the five remaining edges on $\{4,5,6,7\}$ have a unique placement in each of the six embeddings of $K_{3,4}$ and all of five of these edges may be embedded simultaneously. Now there are three possibilities for which edge on $\{1,2,3\}$ is included in F_G, call it e. Any one of these three possibilities for e may exist in exactly two of the six embeddings of $F_G\backslash e$. By symmetry we may therefore assume that e is the $(1,2)$-edge. The two embeddings of $F_G\backslash e$ that extend to all of F_G along with all possible patches are shown in Figure 62. These two embeddings are related by a Q-Twist as shown.

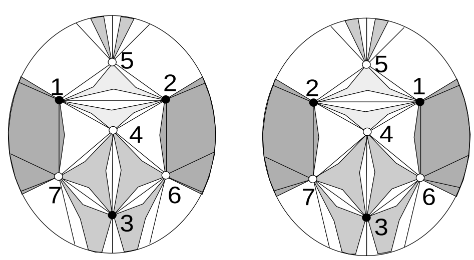

Figure 62.
Flexibility of $\overline{P_2M_1E_2}$ by Q-Twists

Case 2.2 Let $F_G = \overline{P_3M_1E_1}$ where the P_3 is on vertices $6,4,7,5$, in that order. Therefore F_G contains the path on vertices $4,5,6,7$, in that order. Now assume that σ_1 is a patch embedding on F_G with the $K_{3,4}$-subgraph as shown on the top right of Figure 60. This forces the missing edge on vertices $\{1,2,3\}$ to be the $(1,3)$-edge. Now the only other possible embedding of F_G has the $K_{3,4}$-subgraph embedded as on the bottom right of Figure 60. If a second patch embedding σ_2 restricts to the same embedding of the $K_{3,4}$-subgraph, then the only difference between σ_1 and σ_2 is the placement of the $(2,3)$-edge; all other patches and edges have only one possible placement. If σ_2 restricts to the second possible embedding of the $K_{3,4}$-subgraph, then all possible edges and patches along with their possible placements are shown in Figure 63. These embeddings are related by a single Q-Twist hinged at $1,2,3,6$ and latched at $2,5$ and by flipping of single edges edges as shown.

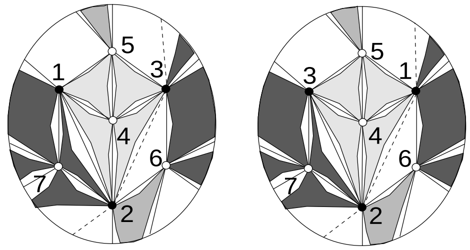

Figure 63.
Flexibility of $\overline{P_3M_1E_1}$ by Q-Twists

Case 2.3 Let $F_G = \overline{P_2P_2E_1}$ where one of the copies of P_2 is on vertices $5, 4, 6$, in that order. Assume we have a patch embedding of F_G with the $K_{3,4}$-subgraph embedded as in the top left of Figure 60. Thus the edge of F_G on vertices $\{1, 2, 3\}$ can either be the $(1, 2)$- or $(2, 3)$-edge. Without loss of generality we assume that it is the $(2, 3)$-edge. Of the six possible embeddings of $K_{3,4}$-subgraph, only four extend to all of F_G and these are shown in Figure 64. Note that the $(2, 3)$-edge has only one possible placement in each of the four possibilities for the $K_{3,4}$-subgraph. Furthermore, any patch has only one possible placement with respect to the embedding of the $K_{3,4}$-subgraph in σ_1. Thus σ_2 restricts to one of the other three embeddings of the $K_{3,4}$-subgraph.

The arrows between the four embeddings on the left of Figure 64 indicate Q-Twist operations relating the two embeddings of F_G. All possible patches in common to the two embeddings in the top row are shown to respect the Q-Twist. The maximal sets of patches for the other embedding of F_G connected by an arrow similarly respects the Q-Twist. All possible common patches for the upper left and lower right embeddings of F_G are shown in the rightmost column of Figure 64. These two patch embeddings are related by a degenerate P-Twist as follows. Take the bowtie view of the P-Twist and contract patches 2,5,8 and contract an edge of patches 7 and 0 to obtain the embeddings in the middle column on the right of Figure 64. These can be seen to be the same as those on in the rightmost column.

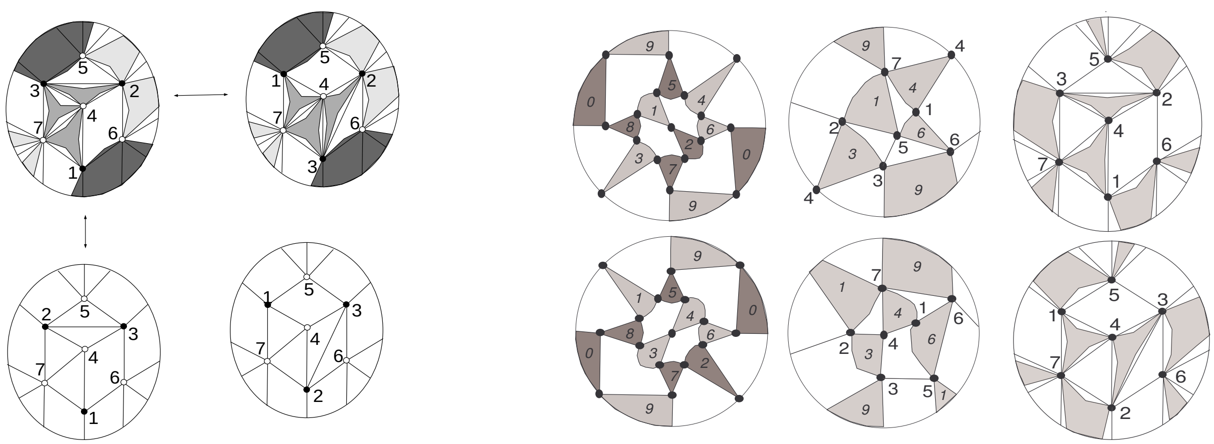

Figure 64.
Possible Patch Structures for $F_G = \overline{P_2P_2E_1}$

Case 2.4 Here $F_G = \overline{P_2P_3}$ when can be obtained from $\overline{P_2P_2E_1}$ in Case 2.3 with the edge $(5, 7)$ deleted. The embeddings of F_G in the projective plane are all obtained from the four embeddings of $\overline{P_2P_2E_1}$ in Case 2.3 with possible reembedding of the $(2, 3)$-edge (see Figure 65. So now any two patch embeddings of F_G are related as they are in Case 2.3 after possible reembedding of the $(2, 3)$-edge.

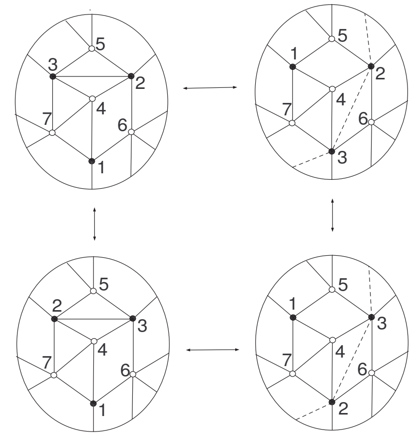

Figure 65.
Flexibility of $\overline{P_2P_3}$ by Q-Twists

Case 2.5 Here $F_G = \overline{P_2M_2}$ where M_2 is the matching $(4,5)$ and $(6,7)$. The edges of the quadrilateral on vertices $4,6,5,7$, in that order, are uniquely embeddable in each of the six embeddings of $K_{3,4}$. Any edge on vertices $\{1,2,3\}$ embeds along with this quadrilateral in exactly two of the six embeddings of $K_{3,4}$. So without loss of generality, we may assume that the $(2,3)$-edge is contained in F_G and in any embedding of F_G, the $(2,3)$-edge may be flipped. Figure 66 shows all of the possible patch embeddings of F_G. These patch embeddings are related by a single Q-Twist along with flipping of the $(2,3)$-edge.

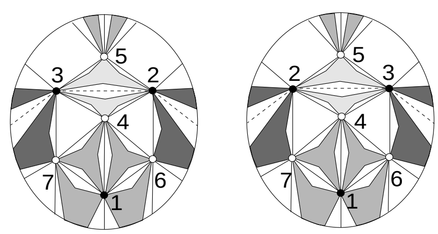

Figure 66.
Flexibility of $\overline{P_2M_2}$ by Q-Twists

5.4.6 Frames that contain $\overline{C_7}$

Now we will consider the flexibility of the graphs in $\mathcal{L}$ that contain a $\overline{C_7}$-subgraph, but no $K_{3,4}$-subgraph. There are four such graphs, $\overline{C_7}, \overline{P_6}, \overline{P_5E_1}$, and $\overline{P_4M_1}$ (see Figure 67). Consider these to be Cases 1–4, respectively.

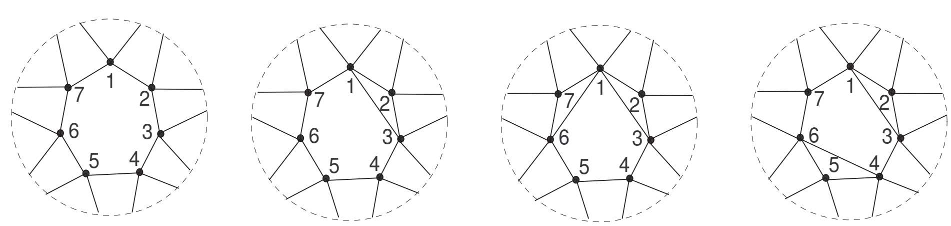

Figure 67.
Graphs $\overline{C_7}, \overline{P_6}, \overline{P_5E_1}$, and $\overline{P_4M_1}$

Case 1 The graph $\overline{C_7}$ has 15 embeddings on the projective plane. To describe them, express $\overline{C_7}$ as an edge-disjoint union of the two 7-cycles: cycle C_1 with edges $(i, i+1)$ for $1 \le i \le 7$ (mod 7) and cycle

C_2 with edges $(i, i+4)$ for $1 \leq i \leq 7 \pmod 7$. It is straightforward to verify that in any embedding C_1 (and also C_2) must be contractible. Furthermore, at most two edges of C_2 can belong to the interior of the C_1-face in any embedding. Moreover, if there are two C_2-edges in the interior of the C_1-face, they then must share a common endpoint. Hence the embeddings of $\overline{C_7}$ fall into three types: the standard embedding with C_2-edges outside the C_1-face; the seven embeddings with a single C_2-edges inside the C_1-face; and the seven embeddings with both C_2-edge incident to vertex i embedded inside the C_1-face. Moving any single edge is done by flipping and so all of these 15 embeddings of $\overline{C_7}$ are related by Q-Twists. This completes Case 1 because any one patch on $F_G \cong \overline{C_7}$, creates a V_8-minor in G. This can be seen as follows. Up to symmetry we may assume there is a patch on $\{1, 4, 5\}$ and so G contains a minor equal to the graph obtained from $\overline{C_7}$ by a ΔY-operation on the triangle $\{1, 4, 5\}$. By inspection one can find a V_8-subgraph.

Case 2 Consider the graph $\overline{P_6}$ that is obtained from $\overline{C_7}$ in Case 1 by adding the $(1, 3)$-edge. Any embedding of $\overline{P_6}$ contains an embedding of $\overline{C_7}$. In the embedding of $\overline{C_7}$ with the $(2, 6)$- and $(2, 5)$-edges flipped into the C_1-face, the $(1, 3)$-edge is embedded outside the C_1-face and in any embedding of $\overline{C_7}$ with the $(2, 6)$- and $(2, 5)$-edges outside the C_1-face, then $(1, 3)$-edge is embedded inside the C_1-face. There are 11 of the 15 embeddings of $\overline{C_7}$ are of the latter type. Moreover, any two of these latter 11 embeddings of $\bar{(}P_6)$ are related by flipping single edges of the C_2-cycle. The former embedding of $\overline{P_6}$ is obtained from the second embedding of Figure 67 hinged at 1,3,5,6 and latched at 2. As in Case 1, if there were a patch attached to a triangle of $\overline{C_7}$, then G would contain a V_8-minor. Hence we need only consider triangles that contain the new edge, $(1, 3)$. There are two such triangles $(1, 3, 4)$ and $(1, 3, 7)$. One can check that a ΔY-operation on either triangle also leads to a V_8-subgraph in G.

Case 3 Consider the graph $\overline{P_5 E_1}$ that is obtained from $\overline{C_7}$ in Case 1 by adding the $(1, 3)$- and $(1, 6)$-edges. If both the $(1, 3)$- and $(1, 6)$-edges are embedded inside the C_1-face, then the remaining embeddings of $\overline{P_5 E_1}$ are obtained from the third embedding of Figure 67 by flippings of the $(1, 4)$-, $(1, 5)$-, and $(3, 6)$-edges. If exactly one of the $(1, 3)$- and $(1, 6)$-edges is embedded outside the C_1-face, then the only such embedding of $\overline{P_5 E_1}$ is obtained from the third embedding of Figure 67 by a Q-Twist with 4 hinges and one latch as in Case 2.

As in Case 2, any patch on $F_G = \overline{P_5 E_1}$ would create a V_8-minor save for the $(1, 3, 6)$-patch. The $(1, 3, 6)$-patch may be added to the third embedding Figure 67 in only one way. Any embedding of F_G with the any of the $(1, 4)$-, $(1, 5)$-, and $(3, 6)$-edges flipped into the C_1-face does not allow for this patch. The $(1, 3, 6)$-patch may be added to either of the remaining two embeddings of F_G in only one way each. This give three patch embeddings. These embeddings are related by full Q-Twists similar to the ones mentioned in the previous paragraph with the second latch at either 3 or 6.

Case 4 Very similar to the reasoning in Case 2.

5.4.7 Frame isomorphic to remaining three graphs on seven vertices

There are only three more graphs in $\mathcal{L}$ to consider. They are $\overline{C_5 E_2}$, $\overline{C_6 E_1}$ and $\overline{B_7}$. The graph $\overline{C_5 E_2}$, however, is the double wheel DW_5 which was analyzed in Section 5.4.2.

Frames isomorphic to $\overline{C_6 E_1}$ The graph $\overline{C_6 E_1}$ consists of a 3-prism plus a seventh vertex adjacent to each of those in the prism. If we label the two triangles of the prism as 1,2,3 and 4,5,6, then one can check that both triangles must be embedded contractibly. Furthermore, the prism cannot be embedded in a disk and so all possible embeddings of $\overline{C_6 E_1}$ are shown in Figure 68 where the dashed lines represent edges with two possible placements. This makes a total of twelve different embeddings.

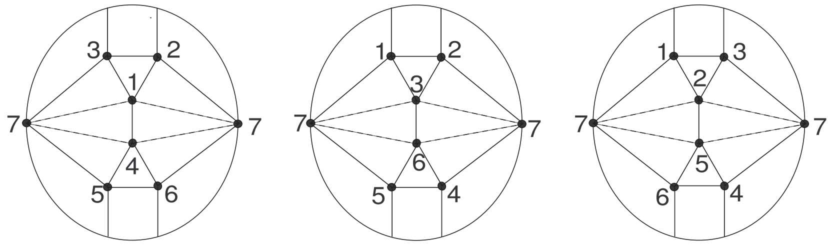

Figure 68.
Possible embeddings of $\overline{C_6E_1}$

Let σ_1 and σ_2 be two different embeddings of G with $F_G \cong \overline{C_6E_1}$. Without loss of generality assume that $\sigma_1|_{F_G}$ is one of the four possible embeddings depicted on the left in Figure 68.

If $\sigma_2|_{F_G}$ is also one of the four possible embeddings depicted on the left in Figure 68, then only possible difference between σ_1 and σ_2 is the placement of a $(1,4,7)$-patch along with flipping of single edges. Thus we can go from σ_1 to σ_2 by at most three Q-Twists.

If $\sigma_2|_{F_G}$ is one of the four possible embeddings depicted in the middle in Figure 68, then the patches that may be placed in both embeddings of F_G are shown in Figure 69. Two patch embeddings may contain all of these patches or some subset of them. In either case, the embeddings shown in Figure 69 are all of the possible patch embeddings save for flipping single edges incident to vertex 7. We can go between the embeddings shown in this figure by a Q-Twist hinged at 5,7,2 and latched at 1,3. The case were $\sigma_2|_{F_G}$ is one of the four possible embeddings depicted on the right in Figure 68, is resolved similarly.

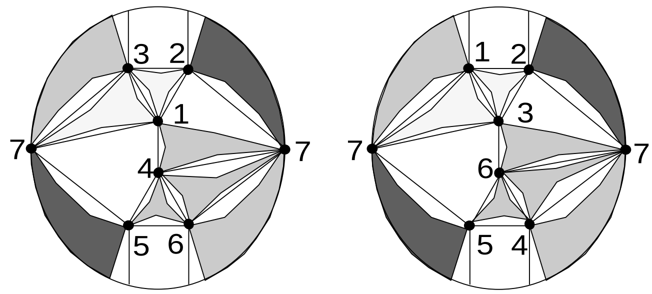

Figure 69.
Maximal patch structure for $\overline{C_6E_1}$

Frame isomorphic to $\overline{B_7}$ Consider the case when the frame graph F_G is isomorphic to $\overline{B_7}$. Let the $K_{3,3}$ subgraph of $\overline{B_7}$ have partite sets $\{1,2,3\}$ and $\{5,6,7\}$ and let the remaining vertex be adjacent to $\{2,3,6,7\}$. The $K_{3,3}$ subgraph can be embedded in exactly six ways. The final vertex 4 can then be embedded in a unique face in four of those embeddings and in one of two faces in the remaining two embeddings. Thus Figure 70 shows all embeddings of $\overline{B_7}$.

Notice that there are only four triangles in $\overline{B_7}$ and hence only four possible patches: $(4,2,6)$, $(4,6,3)$, $(4,3,7)$, and $(4,7,2)$. Furthermore, none of these four possible patches can be embedded in more than one place in any of the eight embeddings of $\overline{B_7}$.

Now in each of the embeddings labeled A, B, C, D, E, or F, all four patches can embed simultaneously as shown in Figure 70. It is straightforward to check that those pairs of embeddings with arrows connecting them are related by Q-Twists. For example, embedding A can be taken to embedding B by a Q-Twist hinged at $5,3,2,7$ and latched at $1,7$.

In embedding H, only the $(4,2,6)$- and $(4,3,7)$-patches may be placed along with F_G. Figure 70 clearly shows that embedding H goes to embedding F by a Q-Twist hinged at 3,7,2,6 and latched at 4. Similarly embeddings G and E with its two possible patches are related by a Q-Twist.

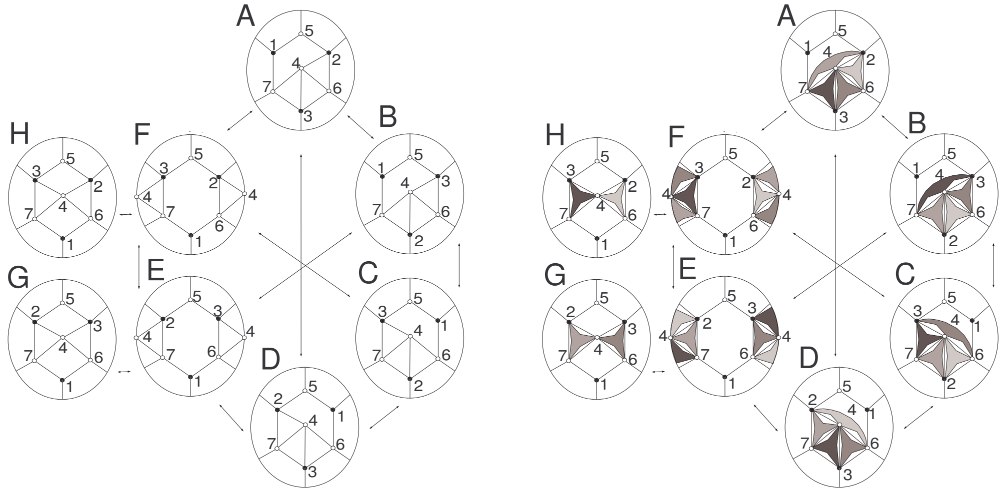

Figure 70.

The eight embeddings of $\overline{B_7}$ with patches

5.4.8 Frames that are 4-vertex coverable graphs

Suppose F_G is a 4-vertex coverable graph on at least 8 vertices. Hence there exist four vertices $a, b, c, d \in V(F_G)$ such that $V(F_G) \setminus \{a, b, c, d\} = \{v_1, v_2, v_3, \ldots, v_t\}$ is independent. If $t < 4$, then F_G would be covered in the previous section. So we may assume that $t \geq 4$. By internal 4-connectivity, each v_i has either three or four neighbors in $\{a, b, c, d\}$. Let $v_1, \ldots, v_m$ have degree four, while $v_{m+1}, \ldots, v_t$ have degree three in G. Note that, as $K_{4,4}$ cannot be embedded in the projective plane, $m \leq 3$. Also note that if two vertices in $v_{m+1}, \ldots, v_t$ have the same three neighbors, those vertices would violate internal 4-connectivity and so $n = t - m \leq 4$.

Suppose $m = 3$ and $n \in \{1, 2, 3, 4\}$, then F_G contains a $K_{3,4}$ subgraph. There is a unique (non-labeled) embedding of $K_{3,4}$ in the projective plane (see Figure 60). By inspection it is not possible to have another vertex adjacent to three of a, b, c, d and so $n = 0$, a contradiction.

Suppose $m = 2$ and $n \in \{2, 3, 4\}$. If $n = 3$, then the bipartite subgraph of F_G with edges from $\{a, b, c, d\}$ to $\{v_1, v_2, v_3, v_4, v_5\}$ contains 17 edges. Euler's formula implies that a bipartite simple graph on the projective plane with v vertices has at most $2v - 2$ edges, and $2v - 2 = 16 < 17$ for $v = 9$, a contradiction. Similarly, we get a contradiction when $n = 4$. So then $m = 2$ and $n = 2$ and say that v_3 is adjacent to a, b, c and v_4 is adjacent to b, c, d. Let B be the induced bipartite subgraph of F_G on partite sets $\{a, b, c, d\}$ and $\{v_1, v_2, v_3, v_4\}$. The only other edges of F_G are on vertices a, b, c, d.

Considering the six possible embeddings of the $K_{3,3}$-subgraph of B on $\{a, b, c, v_1, v_2, v_3\}$, one can see that only two of the six possible embeddings of $K_{3,3}$ extend to an embedding of B and that these extensions are unique (see Figure 71). The only possible edge on $\{a, b, c, d\}$ in $E(F_G) \setminus E(B)$ is (a, d) (shown as a dashed edge in the figure). Any other edge would be in the neighborhood of cubic vertices v_3 or v_4 and these would violate internal 4-connectivity. Now the only possible patches on $F(G)$ are (a, d, v_1) and (a, d, v_2) and the two embedding with both of these patches are related by a single Q-Twist.

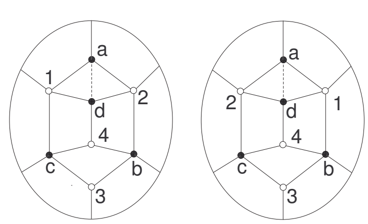

Figure 71.

Flexibility of $K_{4,4} - M_2$

Suppose $m = 1$ and $n \in \{3, 4\}$. If $n = 4$, then F_G contains a $(K_{4,5} - M_4)$-subgraph, which is one of the 35 minor-minimal non-projective planar graphs (see, e.g., [1]). Thus $n = 3$ and so F_G contains a $(K_{4,4} - M_3)$-subgraph on partite sets $\{a, b, c, d\}$ and $\{v_1, v_2, v_3, v_4\}$ with missing edges $(v_1, b), (v_2, c), (v_3, d)$. This subgraph contains all of the edges of F_G except perhaps for any edges on $\{a, b, c, d\}$; however, adding any such edge would violate internal 4-connectivity and so this bipartite subgraph is, in fact, all of F_G. Since the graph is triangle free, there are no patches. Note that this graph is the alternating wheel AW_6 with rim $\{b, v_2, d, v_1, c, v_3\}$ and hubs a and v_4 whose reembeddings are described in Section 5.4.2.

Suppose $m = 0$ and $n = 4$. The subgraph of F_G minus any edges on $\{a, b, c, d\}$ is the cube and we can add all possible edge on $\{a, b, c, d\}$ and remain planar, a contradiction.

5.4.9 Frame isomorphic to the line graph of $K_{3,3}$

There are six embeddings of the line graph of $K_{3,3}$ which correspond to the embeddings of $K_{3,3}$ itself. Topologically the embeddings all look as shown in Figure 72, we show one such embedding. If F_G is isomorphic to the line graph of $K_{3,3}$, then the only patches can be as shown in Figure 72. The six possible embeddings are all related by Q-Twists as with the embeddings of $K_{3,3}$.

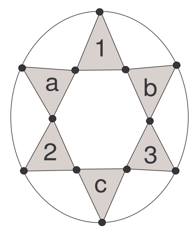

Figure 72.
Patch Structure of $L(K_{3,3})$

6 A review of previous work

Flexibility of embeddings of graphs in the projective plane and its relationship with representativity has been studied previously in several articles, e.g., [3, 4, 10, 19, 20]. In particular, results placing an upper bound on the number of reembeddings of a well-connected graph of a certain representativity have been of interest. In this section we review some of these results, provide counterexamples to some false statements, and provide a new proof where an old one was based on incorrect assumptions.

6.1 Past errors and counterexamples

In [20, Cor.3.1] it is stated that any two distinct 3-representative embeddings of a graph in the projective plane are related by a sequence of Q-Twists, W-Twists, and a degenerate P-Twisting operation that is there called a T-Twist. The line graph of the Petersen graph, $L(P)$, has exactly two distinct embeddings and they are not related by any of these operations. As discussed in Section 2, the two embeddings of $L(P)$ are not related by a Q-Twist. Similarly, the T-Twist operation as shown in [20, p.345] has at most seven vertices whose rotation systems change as a result of the T-Twist operation. Whereas the two embeddings of $L(P)$ have fifteen such vertices. Other counterexamples are obtained by 3-summing graphs onto the triangular faces of $L(P)$. (Such embeddings are depicted in Figure 3.)

In [10, Thm.1.4] it is stated that any two distinct embeddings of a 3-connected graph in the projective plane are reembeddings of one of five different types. Of all of the types described, only one (which is called Type II and is shown in [10, Fig.9]) is for 3-representative embeddings. An inspection of this figure reveals that it is a full Q-Twist. Recall that the full Q-Twist changes an embedding by changing the rotation system at exactly six vertices; again, the two embeddings of $L(P)$ (or $L(P)$ 3-summed with planar graphs on its triangular faces) have changes of rotation at all 15 of its vertices. Another problem is the following. The complete graph K_6 has 12 distinct embeddings in the projective plane, any pair of which are related by a sequence of Q-Twists; however, not all pairs are related by just one Q-Twist as stated in [10, Thm.1.4]. For example, consider the 5-wheel graph W_5 with vertices 1, 2, 3, 4, 5, and h where h is the central hub. An embedding of K_6 in the projective plane is a unique extension of a planar embedding of W_5. Say σ_1 is the embedding of W_5 (i.e., of K_6) with rotation 1,2,3,4,5 for h and σ_2 is the embedding for W_5 with rotation 1,3,5,2,4 for h. The embeddings σ_1 and σ_2 cannot be related by a single Q-Twist because sequence 1,3,5,2,4 is not obtained from 1,2,3,4,5 by reversing a single consecutive substring of digits, which is precisely what a Q-Twist accomplishes.

In [17, Cor.3] it is stated that a 4-connected non-planar graph on at least 11 vertices with a 3-representative embedding in the projective plane has a unique embedding in the projective plane. Again, the two distinct labeled embeddings of $L(P)$ provide a counterexample to this statement.

6.2 Discussion and proof of previous results

In our search of the previous literature, we found two correct results that are based on the incorrect statements in [10] and [20]: Theorem 6.1 (originally stated in [10, Thm. 5.3] and [20, Cor. 3.2]) and Theorem 6.2 (originally stated in [10, Thm. 1.3]).

A correct proof of Theorem 6.1 was given by Robertson and Vitray in [13, Prop. 11.1]. It is worth noting, however, that Theorem 6.1 also follows immediately from Lemma 1.2.

Theorem 6.1. *If G is 3-connected and has a 4-representative embedding in the projective plane, then this embedding is the unique embedding of G in the projective plane.*

Theorem 6.2. *If $G \ncong K_6$, is 5-connected, and has a 3-representative embedding in the projective plane, then this embedding is the unique embedding of G in the projective plane.*

Proof. If we assume that G has two distinct embeddings in the projective plane, then by Lemma 1.2 the flexibilities are accounted for by Q-Twists and P-Twists. We will see that each possibility leads to a contradiction.

In a Q-Twist, any degeneracies lead to a 2-representative embedding and so the Q-Twist is non-degenerate. Now if there is any interior vertex in any one of the three quadrilateral patches of the Q-Twist, then there is a 4-separation of that vertex from one of the hinge or latch vertices, a contradiction. Thus G has exactly 6 vertices that are the hinges and latches of the Q-Twist and since K_6 is minor-minimally 3-representative, $G \cong K_6$.

In a P-Twist or degenerate P-Twist, the patches are all triangular. Any vertex in the interior of a triangular patch is separated from any vertex off of the patch by the three corner vertices of the patch. This is a contradiction of 5-connectivity unless all vertices of G are on this patch. In this case, G would consist of this planar triangular patch and edges outside of the patch connecting the three corners of the patch. One can check that this cannot have a 3-representative embedding, a contradiction. Thus none of the triangular patches of G contain interior vertices and so G is a minor of the line graph of the Petersen graph, $L(P)$. Once we show that K_6 is the only 5-connected minor of $L(P)$, our result will follow.

We actually prove the stronger result that the only minor of $L(P)$ that is simple and with minimum degree at least 5 is K_6. If $|V(G)| = 6$, then we must have that $G \cong K_6$.

If $|V(G)| = 7$, then the only way that the minimum degree of G can be at least 5 is if G has a subgraph isomorphic to K_7 minus a 3-edge matching. This graph, however, is one of the 35 minor-minimal non-projective-planar graphs, a contradiction.

If $|V(G)| = t \geq 8$, then let $C_1, \ldots, C_t$ be the connected components of $L(P)$ that correspond to the vertices of G. Since $t \geq 8$ and $|V(L(P))| = 15$, some C_i consists of a single vertex; however, $L(P)$ is 4-regular which is a contradiction of the fact that G has minimum degree at least 5. □

Acknowledgements

The authors would like to thank the anonymous referees and Mark Ellingham (the managing editor of the Journal of Combinatorial Theory Series B) for their very careful reading of the manuscript and many helpful suggestions to improve the paper.

References

[1] Dan Archdeacon, *A Kuratowski theorem for the projective plane*, J. Graph Theory **5** (1981), no. 3, 243–246.

[2] Martin Juvan, Jože Marinček, and Bojan Mohar, *Elimination of local bridges*, Math. Slovaca **47** (1997), no. 1, 85–92, Graph theory (Donovaly, 1994).

[3] Shigeru Kitakubo and Seiya Negami, *Re-embedding structures of 5-connected projective-planar graphs*, Discrete Math. **244** (2002), no. 1-3, 211–221, Algebraic and topological methods in graph theory (Lake Bled, 1999).

[4] Serge Lawrencenko, *The variety of triangular embeddings of a graph in the projective plane*, J. Combin. Theory Ser. B **54** (1992), no. 2, 196–208.

[5] John Maharry and Neil Robertson, *The structure of graphs not topologically containing the Wagner graph*, submitted for publication.

[6] Bojan Mohar, *Uniqueness and minimality of large face-width embeddings of graphs*, Combinatorica **15** (1995), no. 4, 541–556.

[7] Bojan Mohar and Neil Robertson, *Flexibility of polyhedral embeddings of graphs in surfaces*, J. Combin. Theory Ser. B **83** (2001), no. 1, 38–57.

[8] Bojan Mohar, Neil Robertson, and Richard P. Vitray, *Planar graphs on the projective plane*, Discrete Math. **149** (1996), no. 1-3, 141–157.

[9] Bojan Mohar and Carsten Thomassen, *Graphs on surfaces*, Johns Hopkins Studies in the Mathematical Sciences, Johns Hopkins University Press, Baltimore, MD, 2001.

[10] Seiya Negami, *Re-embedding of projective-planar graphs*, J. Combin. Theory Ser. B **44** (1988), no. 3, 276–299.

[11] James G. Oxley, *Matroid theory*, Oxford Science Publications, The Clarendon Press Oxford University Press, New York, 1992.

[12] Hongxun Qin, Daniel C. Slilaty, and Xianqqian Zhou, *The regular excluded minors for signed-graphic matroids*, Combin. Probab. Comput. **18** (2009), no. 6, 953–978.

[13] Neil Robertson and Richard Vitray, *Representativity of surface embeddings*, Paths, flows, and VLSI-layout (Bonn, 1988), Algorithms Combin., vol. 9, pp. 293–328.

[14] Neil Robertson, Xiaoya Zha, and Yue Zhao, *On the flexibility of toroidal embeddings*, J. Combin. Theory Ser. B **98** (2008), no. 1, 43–61.

[15] P. D. Seymour and Robin Thomas, *Uniqueness of highly representative surface embeddings*, J. Graph Theory **23** (1996), no. 4, 337–349.

[16] Daniel C. Slilaty, *On cographic matroids and signed-graphic matroids*, Discrete Math. **301** (2005), no. 2-3, 207–217.

[17] Yusuke Suzuki, *Re-embedding structures of 4-connected projective-planar graphs*, J. Graph Theory **68** (2011), no. 3, 213–228.

[18] K. Truemper, *Matroid decomposition*, Academic Press Inc., Boston, MA, 1992.

[19] R. P. Vitray, *Representativity and flexibility of drawings of graphs on the projective plane*, Ph.D. thesis, The Ohio State University, 1987.

[20] ———, *Representativity and flexibility on the projective plane*, Graph structure theory (Seattle, WA, 1991), Contemp. Math., vol. 147, Amer. Math. Soc., Providence, RI, 1993, pp. 341–347.

[21] Hassler Whitney, *2-Isomorphic Graphs*, Amer. J. Math. **55** (1933), no. 1-4, 245–254.

[22] ———, *Planar graphs*, Fund. Math. **21** (1933), 73–84.

[23] Thomas Zaslavsky, *Signed graphs*, Discrete Appl. Math. **4** (1982), no. 1, 47–74.